autophosphorylation (*20*, *21*). Forced expression of Dok-7 induced an intense tyrosine phosphorylation of MuSK but not the kinase-inactive mutant with a Lys/Ala substitution (MuSK-KA), indicating that Dok-7 induced the autophosphorylation of MuSK (Fig. 1G). This activity was unique to Dok-7; no other mammalian Dok-family proteins induced phosphorylation of MuSK (fig. S6). It was also conserved; Dok-7 from puffer fish was able to activate even mammalian MuSK. Also, in C2 myotubes, the forced expression of Dok-7 induced tyrosine phosphorylation of MuSK and the β subunit (AChRβ1) of the AChR complex, which is known to be tyrosine-phosphorylated upon activation of MuSK (*22*) (Fig. 1H). Furthermore, this forced expression induced numerous clusters of AChRs, and the number of AChR clusters correlated with the amount of Dok-7 expression plasmid (Fig. 1, I and J; fig. S7A and supporting online material). The exogenous Dok-7–induced AChR clusters were elaborately branched, and their complicated architecture resembled the differentiated "pretzel-like" AChR clusters formed in vivo (fig. S7, B and C). In addition, forced expression in myotubes of Dok-7 that had been fused with enhanced green fluorescent protein (EGFP) induced Dok-7 and AChR coclustering (fig. S7, D to I), as observed at postsynaptic areas in vivo (Fig. 1, C and F).

Because the regulatory interaction of Dok-7 with MuSK as described above implies their physical interaction, we examined whether Dok-7 binds to MuSK by way of the PTB domain in 293T cells. MuSK was coimmunoprecipitated with Dok-7 but not with Dok-7 carrying three Arg/Ala substitutions (Dok-7–RA) in the PTB domain (Fig. 2A). Consistently, the mutant MuSK carrying either a Tyr/Phe substitution at Tyr^{553} (MuSK-YF) or an Asn/Ala substitution at Asn^{550} (MuSK-NA) in the PTB target motif was not coimmunoprecipitated with Dok-7 (fig. S9 and Fig. 2B). The failure of the MuSK-KA kinase-inactive mutant to be coimmunoprecipitated with Dok-7 confirms the requirement of tyrosine phosphorylation for the binding of MuSK with Dok-7 via the PTB domain. These results indicate that Dok-7 binds to MuSK through the PTB domain in a manner dependent on the tyrosine phosphorylation of its target motif in MuSK.

Nevertheless, mutations in the PTB domain (Dok-7–RA) or PTB target motif (MuSK-NA or -YF) did not block activation of MuSK, at least in heterologous cells (Fig. 2, A and B). In addition, the N- and C-terminal deletion mutants of Dok-7 (Dok-7-ΔN and -ΔC) revealed that the C-terminal moiety, but not the PH domain, of Dok-7 is dispensable for MuSK activation in heterologous cells (fig. S10). Also, the forced expression of Dok-7–RA or Dok-7–ΔC induced MuSK activation even in C2 cells at day 3 of differentiation into myotubes (Fig. 2C), when very few myotubes have formed. Unexpectedly, however, the PTB domain and C-terminal portion were indispensable for Dok-7–induced MuSK activation and AChR clustering in fully differentiated C2 myotubes at days 6 and 7 of differentiation (Fig. 2, C and D). In addition, the PH domain, responsible for membrane localization in general, was indispensable for the activation of MuSK in fully differentiated myotubes (fig. S11), as was seen in heterologous cells (fig. S10). Together these findings suggest that a negative regulatory mechanism preventing MuSK activation is established upon differentiation into myotubes, which is accompanied by increased expression of MuSK and Dok-7 (fig. S12). Trace phosphorylation of MuSK in myotubes might allow physical interaction with Dok-7, in turn facilitating dimerization and/or conformational changes in MuSK that are necessary for its sustained activation.

MuSK-deficient myotubes do not form agrin-dependent or -independent clusters of AChRs unless MuSK is reintroduced (*18*, *19*, *23*). To confirm whether Dok-7–mediated AChR clustering is dependent on MuSK, we introduced Dok-7 into MuSK-deficient myotubes. Unlike its effect in C2 myotubes, forced expression of Dok-7 induced no AChR clustering in the MuSK-deficient myotubes; however, additional expression of wild-type MuSK resulted in robust clustering of AChRs in these cells (Fig. 3A). Furthermore, the MuSK-KA and MuSK-YF mutant each failed to complement the MuSK deficiency, regardless of exogenous Dok-7. These findings demonstrate that Dok-7–induced AChR clustering in myotubes depends on Dok-7 interaction with MuSK and subsequent activation of MuSK catalytic activity. Thus, we examined the regulatory interaction of Dok-7 with a MuSK mutant [MuSK-Val/Met (MuSK-VM)] that carries a Val^{790} to Met substitution. This mutation is causally associated with the congenital myasthenic syndrome by way of an as yet unclear mechanism (*24*). As observed with MuSK-YF (Fig. 2B), forced expression of Dok-7 in 293T cells induced the autophosphorylation of MuSK-VM, but its coimmunoprecipitation with Dok-7 was barely detectable in these heterologous cells (fig. S13). Forced expression of Dok-7 with MuSK-VM induced only very weak AChR clustering in MuSK-deficient myotubes (Fig. 3A). Therefore, the congenital myasthenic syndrome–associated Val^{790} to Met mutation impaired interaction of MuSK with Dok-7, suggesting a possible cause of neuromuscular junction dysfunction in these patients.

To examine the effects of Dok-7 down-regulation in myotubes, we used a small interfering RNA (siRNA) designed specifically to block its expression. Inhibition of Dok-7 suppressed the tyrosine phosphorylation of

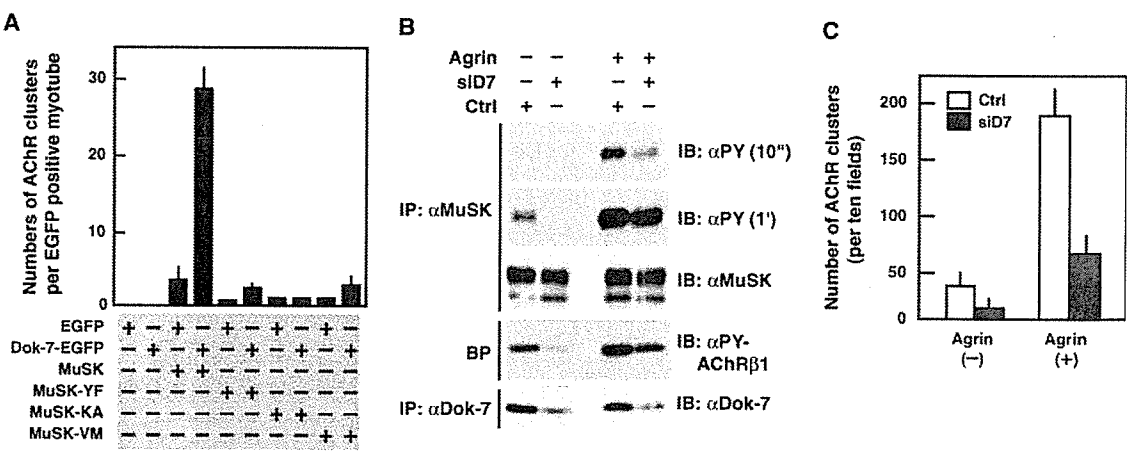

Fig. 3. Dok-7 is essential for activation of the MuSK-pathway to AChR clustering in myotubes. (**A**) MuSK is required for Dok-7–induced AChR clustering. MuSK-deficient myotubes were transfected with the indicated plasmids. The number of AChR clusters (mean ± SD) per EGFP-positive myotube is shown. MuSK-VM is a congenital myasthenic syndrome–associated mutant. (**B**) Activation of the MuSK pathway requires Dok-7. C2 myotubes transfected with Dok-7 siRNA (siD7) or the control (Ctrl) without (−) or with (+) agrin treatment for 15 min were studied as in Fig. 1H. Both short [10 s (10″)] and long [1 min (1′)] exposures are shown for the anti-PY IB of the anti-MuSK IP. (**C**) Dok-7 is essential for AChR clustering. C2 myotubes were transfected with Dok-7 siRNA (siD7) or the control (Ctrl) with or without agrin treatment for 12 hours. The number of AChR clusters (mean ± SD) is shown.

MuSK and AChRβ1 in C2 myotubes, demonstrating its essential role in the aneural, basal catalytic activity of MuSK (Fig. 3B). Indeed, MuSK-dependent spontaneous AChR clustering was suppressed by this siRNA-mediated inhibition (Fig. 3C). Moreover, the inhibition of Dok-7 impaired the agrin-dependent activation of MuSK, the phosphorylation of AChRβ1, and the subsequent formation of AChR clusters (Fig. 3, B and C). Thus, we conclude that Dok-7 is essential for aneural activation of MuSK and AChR clustering in myotubes and is also crucial for agrin-dependent activation of MuSK and AChR clustering. Nonetheless, our results do not exclude the possibility that Dok-7 might also play a role downstream of MuSK. Indeed, Dok-7 and MuSK were synchronously tyrosine phosphorylated upon treatment of myotubes with agrin (fig. S14).

We generated mice lacking Dok-7 to explore its role in vivo (fig. S15). Like mice lacking MuSK or agrin (*6*, *7*), all Dok-7–deficient (Dok-7$^{-/-}$) mice were immobile at birth and died shortly thereafter (26 homozygotes were observed among the first 137 pups), although their wild-type and heterozygous littermates appeared normal. Also, the alveoli of the mutant mice were not expanded at birth (fig. S15D), indicating a failure to breathe and suggesting a severe defect in neuromuscular transmission in the skeletal muscles. Consistently, there were no detectable AChR clusters in the endplate area of the diaphragm muscle in Dok-7$^{-/-}$ embryos at either E14.5 or E18.5 (Fig. 4, E and K). Because nascent AChR clusters are formed in a nerve- and agrin-independent manner at E13.5 to E16.5, whereas most neuromuscular junctions are formed in a nerve- and agrin-dependent manner at E18.5, our findings indicate a requirement for Dok-7 in both types of MuSK-dependent postsynaptic specialization, although we cannot exclude the possibility that nascent AChR clustering is a prerequisite for nerve- and agrin-dependent AChR clustering (*9*–*11*). Consistent with this finding, Dok-7 transcripts were expressed in the endplate area of the diaphragm muscle (fig. S5). In addition, axonal branches extending from the motor nerve trunk were aberrantly long in the endplate area of Dok-7$^{-/-}$ diaphragms at E18.5 and, unlike the controls, did not terminate near the nerve trunk (Fig. 4, G and J). Overall, these pre- and postsynaptic abnormalities are indistinguishable from those found in mice lacking MuSK (*7*), demonstrating an essential role in vivo for Dok-7 in neuromuscular synaptogenesis, a MuSK-dependent vital process.

MuSK-dependent postsynaptic specialization during neuromuscular synaptogenesis appears to be controlled by multiple regulatory mechanisms (*2*, *25*). We have shown that Dok-7 may be a muscle-intrinsic activator of MuSK by demonstrating its essential role in the aneural activation of MuSK and subsequent AChR clustering in cultured myotubes. This conclusion is further supported by our findings that mice lacking Dok-7 showed marked disruption of neuromuscular synaptogenesis that was indistinguishable from the disruption found in MuSK-deficient mice. Thus, neuromuscular synaptogenesis requires Dok-7 within the skeletal muscle. Dok-7 dysfunction may be involved in the pathogenesis of neuromuscular junction disorders.

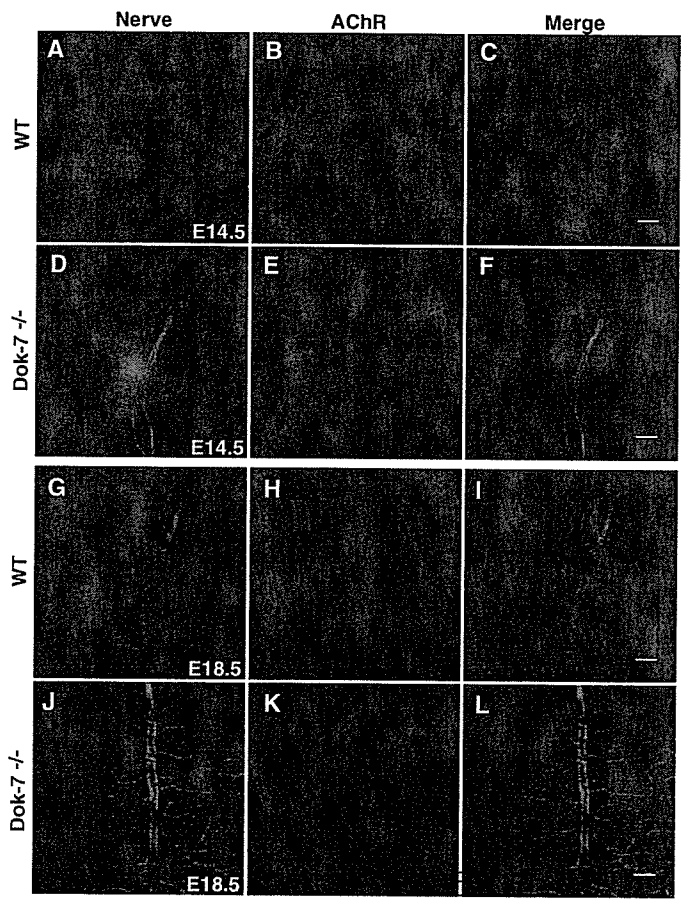

Fig. 4. Dok-7 is essential for neuromuscular synaptogenesis in vivo. Diaphragm muscles were prepared from the wild-type control (WT) or Dok-7$^{-/-}$ embryos at E14.5 (**A** to **F**) or E18.5 (**G** to **L**) and subjected to whole-mount anti-neurofilament and α-bungarotoxin staining, to visualize nerve and AChR, respectively. Scale bars, 100 μm.

References and Notes

1. S. J. Burden, *Genes Dev.* **12**, 133 (1998).
2. J. R. Sanes, J. W. Lichtman, *Nat. Rev. Neurosci.* **2**, 791 (2001).
3. A. G. Engel, K. Ohno, S. M. Sine, *Nat. Rev. Neurosci.* **4**, 339 (2003).
4. A. Vincent *et al.*, *Ann. N. Y. Acad. Sci.* **998**, 324 (2003).
5. D. J. Glass *et al.*, *Cell* **85**, 513 (1996).
6. M. Gautam *et al.*, *Cell* **85**, 525 (1996).
7. T. M. DeChiara *et al.*, *Cell* **85**, 501 (1996).
8. M. Gautam *et al.*, *Nature* **377**, 232 (1995).
9. W. Lin *et al.*, *Nature* **410**, 1057 (2001).
10. X. Yang *et al.*, *Neuron* **30**, 399 (2001).
11. X. Yang, W. Li, E. D. Prescott, S. J. Burden, J. C. Wang, *Science* **287**, 131 (2000).
12. T. Misgeld, T. T. Kummer, J. W. Lichtman, J. R. Sanes, *Proc. Natl. Acad. Sci. U.S.A.* **102**, 11088 (2005).
13. W. Lin *et al.*, *Neuron* **46**, 569 (2005).
14. R. Herbst, E. Avetisova, S. J. Burden, *Development* **129**, 5449 (2002).
15. N. Carpino *et al.*, *Cell* **88**, 197 (1997).
16. Y. Yamanashi, D. Baltimore, *Cell* **88**, 205 (1997).
17. R. J. Crowder, H. Enomoto, M. Yang, E. M. Johnson Jr., J. Milbrandt, *J. Biol. Chem.* **279**, 42072 (2004).
18. H. Zhou, D. J. Glass, G. D. Yancopoulos, J. R. Sanes, *J. Cell Biol.* **146**, 1133 (1999).
19. R. Herbst, S. J. Burden, *EMBO J.* **19**, 67 (2000).
20. A. Watty *et al.*, *Proc. Natl. Acad. Sci. U.S.A.* **97**, 4585 (2000).
21. S. K. H. Gillespie, S. Balasubramanian, E. T. Fung, R. L. Huganir, *Neuron* **16**, 953 (1996).
22. C. Fuhrer, J. E. Sugiyama, R. G. Taylor, Z. W. Hall, *EMBO J.* **16**, 4951 (1997).
23. J. E. Sugiyama, D. J. Glass, G. D. Yancopoulos, Z. W. Hall, *J. Cell Biol.* **139**, 181 (1997).
24. F. Chevessier *et al.*, *Hum. Mol. Genet.* **13**, 3229 (2004).
25. T. T. Kummer, T. Misgeld, J. R. Sanes, *Curr. Opin. Neurobiol.* **16**, 74 (2006).

26. We thank Regeneron Pharmaceuticals for MuSK-deficient cells; K. Manji, J. Hamuro, H. Moriya, and A. Ishii for technical assistance; and M. Shirakata, T. Yasuda, S. Sugano, T. Tezuka, R. F. Whittier, S. Tronick, and T. Yamamoto for discussions. This work was supported by Grants-in-Aid for Scientific Research from the Ministry of Education, Culture, Sports, Science and Technology and by a grant from the Uehara Foundation.

Supporting Online Material

www.sciencemag.org/cgi/content/full/312/5781/1802/DC1
Materials and Methods
SOM Text
Figs. S1 to S15
References

8 March 2006; accepted 19 May 2006
10.1126/science.1127142

Research article

Open Access

Identification of arthritis-related gene clusters by microarray analysis of two independent mouse models for rheumatoid arthritis

Noriyuki Fujikado, Shinobu Saijo and Yoichiro Iwakura

Center for Experimental Medicine, Institute of Medical Science, University of Tokyo, 4-6-1 Shirokanedai, Minato-ku, Tokyo 108-8639, Japan

Corresponding author: Yoichiro Iwakura, iwakura@ims.u-tokyo.ac.jp

Received: 25 Jan 2006 Revisions requested: 16 Feb 2006 Revisions received: 11 May 2006 Accepted: 2 Jun 2006 Published: 28 Jun 2006

Arthritis Research & Therapy 2006, **8**:R100 (doi:10.1186/ar1985)
This article is online at: http://arthritis-research.com/content/8/4/R100

Abstract

Rheumatoid arthritis (RA) is an autoimmune disease affecting approximately 1% of the population worldwide. Previously, we showed that human T-cell leukemia virus type I-transgenic mice and interleukin-1 receptor antagonist-knockout mice develop autoimmunity and joint-specific inflammation that resembles human RA. To identify genes involved in the pathogenesis of arthritis, we analyzed the gene expression profiles of these animal models by using high-density oligonucleotide arrays. We found 1,467 genes that were differentially expressed from the normal control mice by greater than threefold in one of these animal models. The gene expression profiles of the two models correlated well. We extracted 554 genes whose expression significantly changed in both models, assuming that pathogenically important genes at the effector phase would change in both models. Then, each of these commonly changed genes was mapped into the whole genome in a scale of the 1-megabase pairs. We found that the transcriptome map of these genes did not distribute evenly on the chromosome but formed clusters. These identified gene clusters include the major histocompatibility complex class I and class II genes, complement genes, and chemokine genes, which are well known to be involved in the pathogenesis of RA at the effector phase. The activation of these gene clusters suggests that antigen presentation and lymphocyte chemotaxis are important for the development of arthritis. Moreover, by searching for such clusters, we could detect genes with marginal expression changes. These gene clusters include schlafen and membrane-spanning four-domains subfamily A genes whose function in arthritis has not yet been determined. Thus, by combining two etiologically different RA models, we succeeded in efficiently extracting genes functioning in the development of arthritis at the effector phase. Furthermore, we demonstrated that identification of gene clusters by transcriptome mapping is a useful way to find potentially pathogenic genes among genes whose expression change is only marginal.

Introduction

Rheumatoid arthritis (RA) is a systemic, chronic inflammatory disease primarily affecting the joints. The synovial inflammation leads to cartilage destruction, bone erosion, joint deformity, and loss of joint function [1]. This disease is autoimmune in nature and characterized by the infiltration of T cells, B cells, macrophages, and neutrophils into the synovial lining and fluid of the periarticular spaces [2]. The infiltrating cells express adhesion molecules and produce a variety of inflammatory cytokines and chemokines to contribute to the complex pathogenesis of RA. The etiopathogenesis of this disease has not yet been completely elucidated.

Using gene-manipulating techniques, we have established two mouse models for RA: human T-cell leukemia virus type I (HTLV-I)-transgenic (Tg) mice and interleukin-1 receptor antagonist (IL-1Ra)-knockout (KO) mice [3,4]. HTLV-I is the causative agent of adult T-cell leukemia. The virus encodes a

CIA = collagen-induced arthritis; Csf2rb = colony-stimulating factor 2 receptor beta; DC = dendritic cell; EST = expressed sequence tag; GM-CSF = granulocyte-macrophage colony-stimulating factor; HTLV-I = human T-cell leukemia virus type I; Ig = immunoglobulin; IL-1Ra = interleukin-1 receptor antagonist; KO = knockout; KS = knockout severe; MHC = major histocompatibility complex; MMP = matrix metalloproteinase; Ms4a = membrane-spanning four-domains, subfamily A; PGIA = proteoglycan-induced arthritis; RA = rheumatoid arthritis; SAM = significance analysis of microarrays; SD = standard deviation; Tg = transgenic; TS = transgenic severe.

transcriptional transactivator, Tax, within the *pX* region that activates multiple cellular genes, including those for cytokines, cytokine receptors, and immediate early transcriptional factors, via activation of enhancers such as cAMP-responsive enhancer, nuclear factor kappa B-dependent enhancers, or serum-responsive elements [5,6]. Tg mice carrying the *tax* gene spontaneously develop autoimmune arthritis, likely due to overexpression of proinflammatory cytokines and increased T-cell resistance to Fas-induced apoptosis [2,3,7]. IL-1Ra is a negative regulator of IL-1 which competes for the binding of IL-1α and IL-1β to its cognate receptors. Because the three isoforms of IL-1Ra protein, which possess inhibitory activity against IL-1, are synthesized by alternative splicing of a single gene, we produced mice deficient in all three isoforms of IL-1Ra. These IL-1Ra-KO mice also spontaneously develop autoimmune arthritis, due to excess T-cell activation [2,4,8].

Although the etiology of the arthritis differs between these mice, the histopathologies of the lesions are very similar. These lesions exhibit marked synovial and periarticular inflammation, with articular erosion caused by the invasion of granulation tissues, which closely resembles RA in humans. Osteoclast activation is obvious at the pannus, and the infiltration of inflammatory cells, including neutrophils, lymphocytes, and macrophages, can be detected in synovial tissues. Both of these mouse models develop autoimmunity with elevated antibody titers against immunoglobulin (Ig) G and type II collagen. Given that the histopathology observed in these models closely resembles that seen in RA in humans, pathogenic mechanisms similar to those operating in these models are likely functioning in human RA. Actually, an etiological correlation was suggested between HTLV-I and RA in Japan [9,10]. In addition, an association was suggested between IL-1Ra polymorphism and RA [11,12]. We took advantage of these mouse models of RA to analyze comprehensively the gene expression patterns functioning in this condition, using high-density oligonucleotide arrays.

In this analysis, we focused on genes that exhibited similar changes in both of the disease models. This approach should efficiently identify the genes involved in the pathogenesis of arthritis irrespective of the etiology, and these genes should include those that function in the effector phase of inflammation or in the bone erosion process. To determine the genomic distribution of the arthritis-related genes, we assigned these genes into the whole genome. The members of the same gene family often form clusters on the chromosomes [13,14]. Furthermore, because relatively wide genomic regions form open complex structures upon activation [15,16], we expected that genes in the same cluster might be functionally related. Using this analysis, we identified several arthritis-related gene clusters in the specific genomic regions, and some of the genes were successfully detected as a cluster whose expression changes are only marginal.

Materials and methods

Mice

Two mouse models were used for gene expression profiling studies. HTLV-I-Tg mice, originally produced by injection of the LTR-*env-pX*-LTR region of the HTLV-I genome into a (C3H/Hen x C57BL/6J) F_1 embryo [3], were backcrossed to BALB/cA mice (CLEA Japan, Inc., Tokyo, Japan) for 20 generations. These mice start to develop arthritis spontaneously at 4 weeks of age, and 60% and 80% of the mice are affected at 3 months and 6 months of age, respectively. In this study, severely arthritic (score 3) HTLV-I-Tg mice (TS) (females, 6 to 9 weeks of age) were used. Wild-type (WT) littermates were used as controls. IL-1Ra-KO mice, generated by homologous recombination as described previously [4], were backcrossed to BALB/cA mice for eight generations. These mice develop arthritis spontaneously at 5 weeks of age. Eighty percent and almost 100% of the mice became arthritic by 8 and 13 weeks of age, respectively. In this study, IL-1Ra-KO mice (male, 13 weeks of age) that suffered from severe arthritis (score 3) (KS) were used; WT littermates were used as controls. The severity of arthritis was graded for each paw on a scale of 0 to 3 for the degree of redness and swelling: grade 0 = normal; grade 1 = light swelling of the joint and/or redness of the footpad; grade 2 = obvious joint swelling; and grade 3 = severe swelling and fixation of the joint. All mice were kept under specific pathogen-free conditions in an environmentally controlled clean room at the Center for Experimental Medicine, Institute of Medical Science, University of Tokyo. Experiments were conducted according to the institutional ethical guidelines for animal experimentation and the safety guidelines for gene manipulation.

Preparation of total RNA and poly (A)$^+$ RNA from joints

After removal of the skin and muscle, portions of the leg containing the knee, ankle, and finger joints were rapidly frozen in liquid nitrogen. Frozen joints were homogenized using a physcotron (Microtech, Chiba, Japan). Total RNA was extracted from the joint homogenate using the acid guanidium thiocyanate/phenol chloroform extraction method. To avoid fluctuation between individuals, total joint RNAs were pooled from three (TS) or five (KS) arthritic mice and five or six (WT) normal mice for replicates; poly (A)$^+$ RNA was purified on oligo (dT)-cellulose columns. RNA quality was confirmed by spectrophotometry and electrophoresis on formaldehyde gels.

Microarray analysis

A Murine Genome U74v2 Set (GeneChip® system; Affymetrix, Santa Clara, CA, USA) consisting of three GeneChip probe arrays containing approximately 36,000 oligonucleotide probe sets (6,000 full-length mouse genes and 30,000 expressed sequence tag (EST) clusters from the UniGene database) was used for the analysis. Sample labeling and processing were performed according to the manufacturer's protocol. In brief, double-stranded complementary DNA was synthesized, and biotinylated cRNA was prepared and then hybridized to the

Figure 1

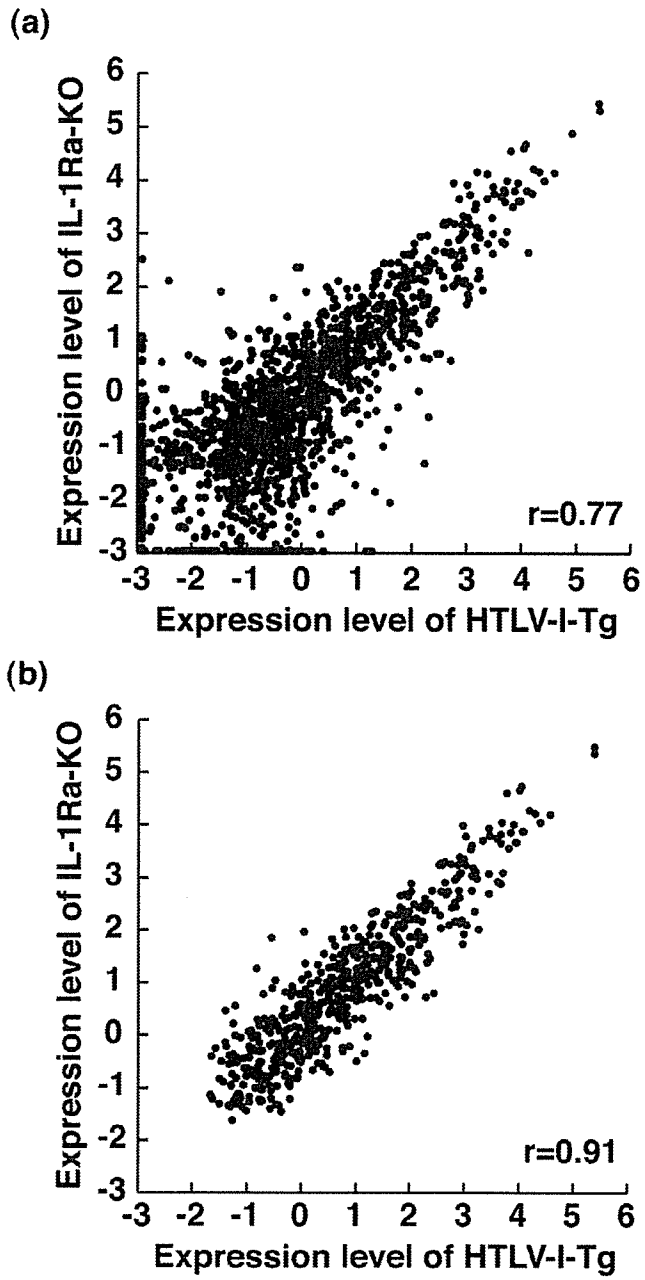

The relationship of gene expression levels between human T-cell leukemia virus type I- transgenic (HTLV-I-Tg) and interleukin-1 receptor antagonist-knockout (IL-1Ra-KO) mice. **(a)** The reciprocal relationship between log-transformed (base 2) normalized gene expression levels for the two models was plotted. The correlation coefficient of gene expression between HTLV-I-Tg and IL-1Ra-KO mice is $r = 0.77$. **(b)** Commonly activated genes were extracted in different models using the SAM (significance analysis of microarrays) method; their relationship is shown. The correlation coefficient is $r = 0.91$.

GeneChip sets. Fluorescent hybridization signals were developed with phycoerythrin-conjugated streptavidin. Fluorescent signals were collected by laser scan, and the results were analyzed with GENECHIP ANALYSIS software (Affymetrix).

Figure 2

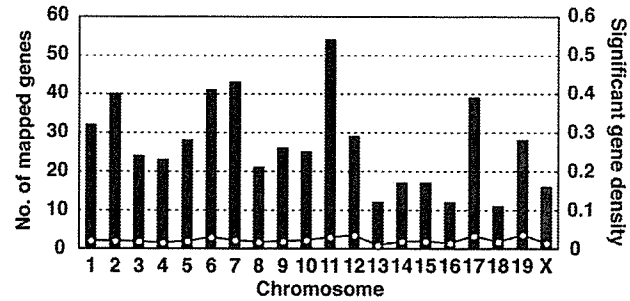

Distribution of arthritis-related genes on the mouse genome. The numbers of significantly changed genes are indicated for each chromosome (closed bars). The density of significantly changed genes (Number of significantly changed genes/Total number of genes on the chromosome estimated from the data of Mouse Genome Search in The Bioinformatics Analytical Toolkit; see Materials and methods) is shown for each chromosome (open circles).

Northern blot hybridization analysis

Tissues were quickly frozen in liquid nitrogen and stored at -80°C. Frozen tissues were homogenized with a physcotron (Microtech). Total RNA was isolated from tissue homogenates by an acid guanidium thiocyanate-phenol-chloroform extraction method, and poly $(A)^+$ RNA was purified using an oligo (dT)-cellulose column. The poly $(A)^+$ RNA was extracted from the paws of four to five mice. Then, the poly $(A)^+$ RNA was electrophoresed on a 1.3% denatured agarose gel and transferred to a nylon membrane (Gene Screen Plus; NEN Life Science, Boston, MA, USA). Hybridization was performed at 42°C overnight with ^{32}P-labeled DNA probes labeled with Megaprime DNA labeling system (GE Healthcare, Little Chalfont, Buckinghamshire, UK) and ^{32}P-dCTP (3,000 Ci/mmol; NEN Life Science). The radioactivity was measured using the BAS-2000 system (Fuji Photo Film Co., Tokyo, Japan).

Statistical analysis and data management

Data were normalized by the average fluorescent intensities for each microarray experiment, and expression values based on the perfect match/mismatch model were calculated for each GeneChip. For the pairwise comparison between normal mice and arthritic mice, signals were filtered using several criteria. The following gene sets were selected: (a) the gene was present in the arthritic mice but absent in the normal mice, (b) the gene was present in the normal mice but absent in the arthritic mice, and (c) the gene was present in both arthritic mice and normal mice. Fold changes for gene expression were calculated, and genes with more than a threefold change in gene expression were selected for further characterization. We assumed that the same group of genes is involved in the pathogenesis of arthritis in both models, and we extracted commonly changed genes in both models. To extract commonly changed genes, we applied the principle of the significance analysis of microarrays (SAM) method [17] for the statistical analysis of the microarray data. SAM assigns a

Table 1

Identified arthritis-related gene clusters by transcriptome mapping

ID	Chr.	Position (Mb)	*n* of genes	* *n* of total genes	Included gene families
1	17	33	10	48	MHC class II
2	17	34	8	67	Complement
3	17	35	2	40	MHC class I
	17	33–35	20	155	MHC class II/Complement/MHC class I
4	11	81	3	10	CC chemokine ligand
5	11	82	5	25	Schlafen
6	11	83	3	23	CC chemokine ligand
	11	81–83	11	58	Schlafen/CC chemokine ligand
7	6	68	3	19	Immunoglobulin kappa chain
8	6	69	4	16	Immunoglobulin kappa chain
9	6	70	2	13	Immunoglobulin kappa chain
	6	68–70	9	48	Immunoglobulin kappa chain
10	12	112	4	8	Immunoglobulin heavy chain
11	12	113	2	3	Immunoglobulin heavy chain
	12	112–113	6	11	Immunoglobulin heavy chain
12	6	124	5	23	Complement/C-type lectin superfamily
13	15	79	5	27	Colony stimulating factor 2 receptor, beta
14	19	11	5	32	Membrane spanning four-domain, subfamily A
15	2	165	4	32	-
16	3	146	4	10	Guanylate nucleotide binding protein
17	17	17	4	11	Formyl peptide receptor
18	19	5	4	45	-
19	1	75	3	15	-
20	1	167	3	16	Selectin
21	1	174	3	20	(Fc receptor)
22	2	91	3	26	-
23	2	129	3	18	-
24	4	131	3	18	-
25	5	136	3	38	-
26	7	3	3	28	Paired-Ig-like receptor
27	7	37	3	46	-

Table 1 *(Continued)*

Identified arthritis-related gene clusters by transcriptome mapping

28	7	39	3	29	Serum amyloid A
29	7	120	3	30	-
30	9	126	3	15	CC chemokine receptor
31	11	70	3	30	-
32	11	102	3	37	-
33	11	114	3	33	-
34	11	117	3	23	-
35	15	105	3	25	-
36	19	12	3	33	-
37	X	63	3	40	-

*Numbers of total genes in the corresponding 1 megabase were obtained from a Mouse Genome Search in The Bioinformatics Analytical Toolkit [20]. CC, Cysteine-Cysteine type; Chr., chromosome; Fc, Fragment crystallizable; ID, identification number; Ig, immunoglobulin; Mb, megabase; MHC, major histocompatibility complex.

score, $d(i)$, to each gene on the basis of changes in gene expression relative to the standard deviation (SD) of repeated measurements. The 'relative difference', $d(i)$, in gene expression is defined as:

$$d(i) = \frac{\bar{x}_A(i) - \bar{x}_N(i)}{s(i) + s_0}$$

where $\bar{x}_A(i)$ and $\bar{x}_N(i)$ are the average expression levels of a gene (i) in subjects A (arthritis) and N (normal), respectively. The 'gene-specific scatter', $s(i)$, is the SD of the expression measurements. At low expression levels, the variance $d(i)$ can be high because of the small values of $s(i)$. To avoid this, SAM defines a small positive constant, s_0, in the denominator of the above equation. For the present data, computation yielded $s_0 = 0.11$. The $d(i)$ is calculated for each gene, and significance levels are indicated by the q value. The q value is the lowest false discovery rate, the probability of being identified by chance [17]. To assess the reliability of the data, the mean values of the fold change and SD were calculated for the genes that were more than two in the selected gene sets. The range of variance was estimated by calculating ratios of SD to fold change. Forty genes exhibited duplicate or triplicate clones. A conservative approach of interval estimation was used to estimate the dispersion of the fold-change values. The estimated ratio was 0.20 (95% confidence interval, 0.15 to 0.25). This result signifies that the fold-change data fluctuated approximately 20% in this study.

Gene mapping

Using the public genome database [18], SOURCE database [19], and Mouse Genome Search in The Bioinformatics Analytical Toolkit [20], we identified the chromosome and the genomic position at which the genes localized for 538 of the 554 significant genes. Gene cluster scanning was performed in each 1-megabase (Mb) window. Hierarchical clustering was applied using 'Cluster' software, and the results were visualized with 'Treeview' software (M. Eisen at Stanford University, Stanford, CA)[21,22].

Results

Gene expression profiles of synovial tissues from RA model mice compared with normal control mice

We isolated mRNA from the joints of two arthritic models (HTLV-I-Tg and IL-1Ra-KO mice) and normal WT mice. Isolated RNAs were labeled and hybridized to microarrays containing the oligonucleotide probes of approximately 36,000 mouse genes and ESTs from the UniGene database. In this microarray system, each gene is represented as 16 distinct pairs of 25-mer oligonucleotide probes. The mismatch oligonucleotide provides an estimate of the background hybridization signal. Fluctuation of the fold-change data of the genes that were spotted more than once on the array was only 20% (see Materials and methods). Therefore, these arrays allow highly reproducible quantification of gene expression levels. We set the threshold at threefold change, which is well above the fluctuation. We performed two independent experiments for control mice, using independently pooled mRNA preparations from five and six mice, respectively, and the reproducibility was confirmed. Fluctuation between two experiments was approximately 11%. For arthritic mice, mRNA was prepared from three HTLV-I-Tg mice and five IL-1Ra-KO mice, respectively. Accordingly, we selected 1,467 genes, for which the transcript levels changed at least threefold in one of either model from that of the corresponding WT normal mice (Additional File 1). When the log-transformed (base 2) normalized intensities of gene expression levels in HTLV-I-Tg mice were plotted against those of IL-1Ra-KO mice, we observed a high degree of correlation (correlation coefficient, $r = 0.77$),

Figure 3

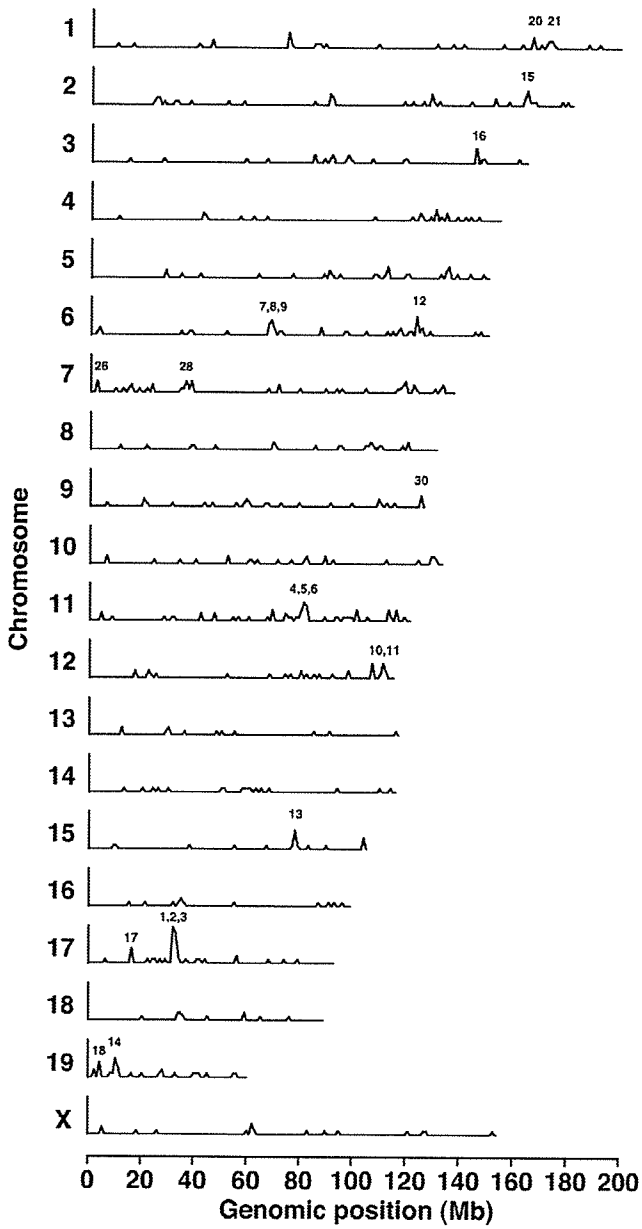

Transcriptome mapping of arthritis-related genes. Significantly changed genes were mapped in every 1-megabase (Mb) interval on each chromosome. The chromosome number is indicated in each panel; the peak number corresponds to the number given in Table 1.

indicating that the expression of many genes changed in both models (Figure 1).

We thought that the same group of genes should be involved in the development of arthritis in both models at the effector phase because the pathology of the disease is very similar between two models. We searched for genes for which the expression levels in the joints changed significantly in both models in comparison with those seen in normal joints, by

Figure 4

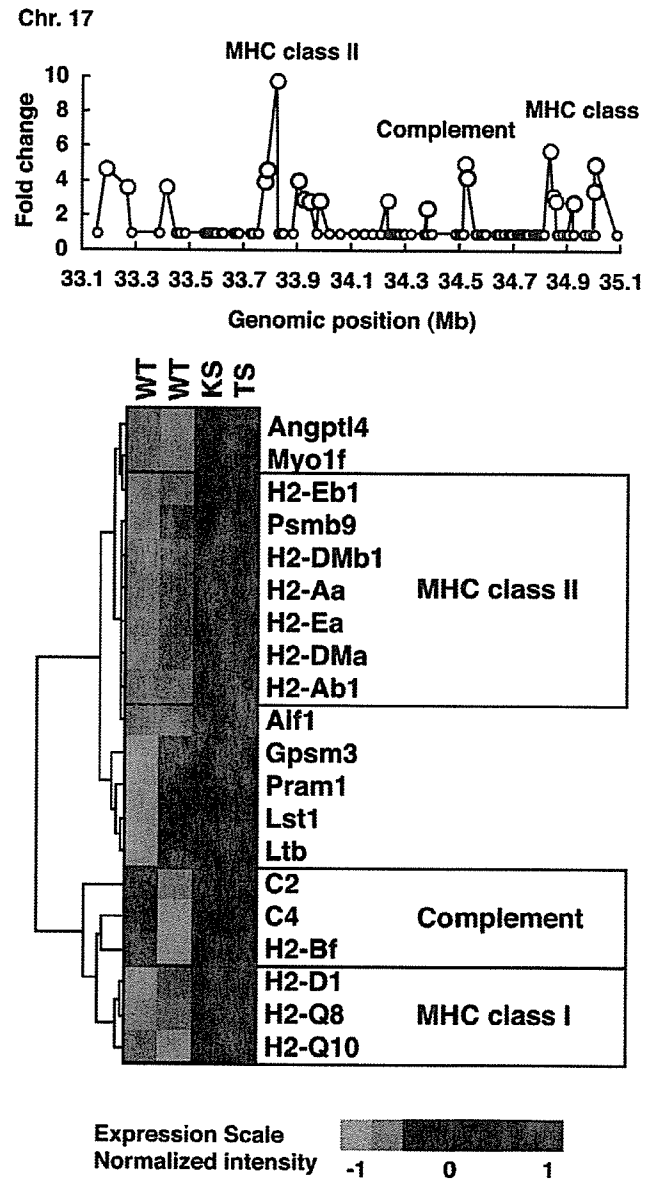

Identification of the *H-2* gene cluster as one of the significantly activated gene clusters. The maximal gene density was mapped to the chromosome (Chr.) 17, 33- to 35-megabase (Mb) locus (#1–3), which corresponds to the *H-2* gene cluster. Fold changes of the significantly changed genes are shown in a region of 2-Mb window. Hierarchical clustering of these genes is visualized below. Each column represents an RNA preparation from a different mouse strain, and each row represents an individual gene. Red represents expression levels greater than the median, and green represents those less than the median. The expression scale is shown at the bottom. KS, interleukin-1 receptor antagonist-knockout mice; MHC, major histocompatibility complex; TS, human T-cell leukemia virus type I- transgenic mice; WT, wild-type mice.

applying the principle of the SAM method and assuming that genes that function during the effector phase would be similarly activated in both models despite the differences in etiol-

Figure 5

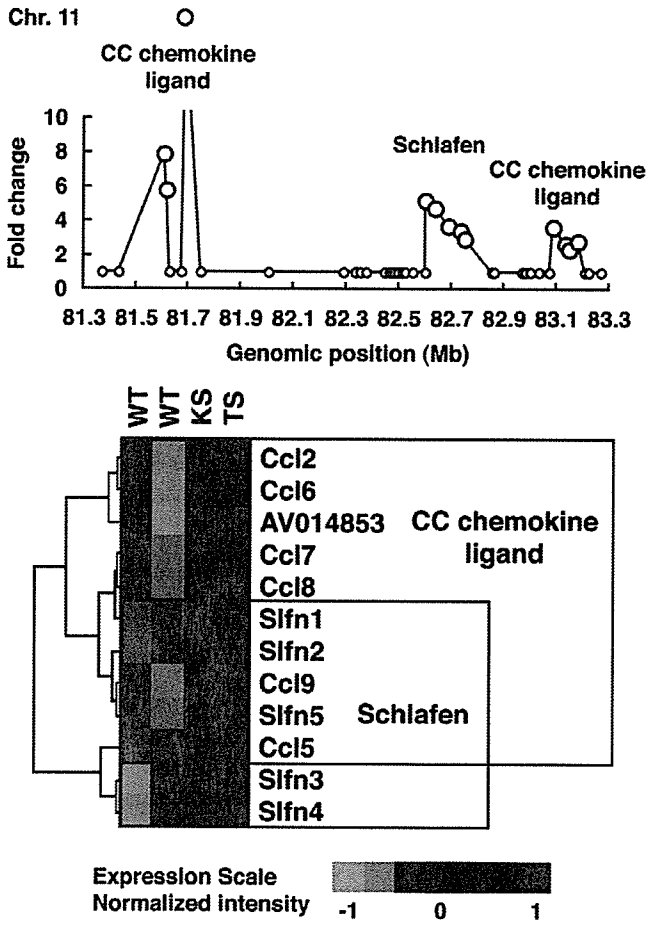

Arthritis-related gene clusters on chromosome (Chr.) 11. The peak at the Chr. 11, 81- to 83-megabase (Mb) (#4–6) includes *Ccl* and *Slfn* family clusters. An expanded view of this region in 2-Mb window is shown. Hierarchical clustering patterns of the expression levels are shown below. *Ccl* and *Slfn* genes are clearly clustered in specific narrow loci and augmented in arthritis. CC, Cysteine-Cysteine type; KS, interleukin-1 receptor antagonist-knockout mice; TS, human T-cell leukemia virus type I- transgenic mice; WT, wild-type mice.

ogy. The fold change in expression for each gene and the significance levels (*q* values) were estimated based on SAM, assuming that the gene expression profiles were identical between two models. A large population of 594 spots was significantly enhanced, and four spots were suppressed, indicating that the expression levels of these genes changed in both models. Because a number of the spots on the array contained oligonucleotides derived from different clones of the same gene, these spots were found to include a total of 554 non-redundant genes (Additional File 2). The log-transformed (base 2) normalized expression intensities of HTLV-I-Tg mice were then plotted against those of IL-1Ra-KO mice (Figure 1b). The gene expression levels of HTLV-I-Tg mice and IL-1Ra-KO mice were quite similar with a high correlation coefficient ($r = 0.91$), supporting the assumption that a panel of specific genes was similarly activated in both RA models and successfully extracted common, differentially expressed genes.

Genes overexpressed in the synovial tissues of RA model mice

The expression of *Saa3* increased maximally (approximately 62-fold) in this study. *Saa1* and *Saa2*, members of the same family, were also significantly upregulated. Many chemokine genes were also activated, including *Cxcl5* (LIX/human ENA-78), *Cxcl1* (KC/human Gro-α), *Cxcl13* (BLC), *Ccl8* (MCP-2), *Ccl7* (MCP-3), *Ccl2* (MCP-1), *Cxcl14* (MIP-2γ), *Ccl5* (RANTES), *Cxcl16* (SR-PSOX), *Ccl9* (Mip-1γ), *Ccl6* (C10), and *Cxcl12* (SDF-1). Genes encoding chemokine receptors, such as *Ccr5*, *Ccr6*, *Ccr1*, *Ccr2*, *Cxcr2* (IL-8Rβ), and *Cxcr4*, were also enhanced significantly. The proinflammatory cytokine *Il1b* (IL-1β) and its receptor *Il1r1* (CD121a) were upregulated. Although the expression of multiple cytokine receptors, including *Tnfrsf1b* (TNF-αR/CD120b),*Il6ra* (CD126), *Il17r* (CDw217), *Il4ra* (CD124), *Ifnar2* (IFN-α/βR), *Csf2rb1* (commonβ/CDw131), *Csf2rb2* (granulocyte-macrophage colony-stimulating factor [GM-CSF]/IL-3R), and *Csf3r* (G-CSFR/CD114), increased, expression of their ligands could not be detected by our analysis. TNF and TNF-R family genes, such as *Tnfsf3* (LTβ), *Tnfsf11* (RANKL/ODF), *Tnfsf31* (Pglyrp), *Tnfrsf5* (CD40), and *Tnfrsf21* (DR6), were significantly elevated. The expression of genes encoding growth factor and growth factor-related proteins, including *Mdk*, *Il18bp*, *Grn*, *Tnfaip6*, *C1qtnf6*, *Fgf10*, *Igf1*, *Igfbp4*, *Igfbp7*, *Pdgfrl*, and *Bmp1*, were also enhanced. In addition to these chemokine/chemokine receptor and cytokine/cytokine receptor genes, several genes were identified that were upregulated more than 10-fold in comparison with WT mice. These genes include *Igh-4* (Serum IgG1) and *Mmp3* (Stromelysin-1), which are transcripts known to be increased in RA [23,24]. Although the expression of *Glipr2*, *Kcnj15*, and *Col4a2* were also elevated, no augmentation of these genes has been previously reported in patients with RA. Moreover, major histocompatibility complex (MHC) class I genes (*H2-D1*,*H2-Q8*, and *H2-Q10*) and MHC class II genes (*H2-DMa*, *H2-DMb1*, *H2-Aa*, *H2-Ab1*, *H2-Ea*, and *H2-Eb1*) were also significantly detected in this data set. Using northern blot hybridization techniques, we examined the expression of some of these genes, including key cytokines and cytokine receptors (*Il1b*,*Il1r1*,*Il-6ra*), chemokines and their receptors (*Cxcl5*,*Cxcl1*,*Cxcr4*), class I and class II MHC genes, and several selected genes, and confirmed the augmented expression of these genes ([3,4] and unpublished data about novel genes).

Density of the arthritis-related genes within each chromosome

Many functionally related genes form clusters on chromosomes [25]. Because these functionally related genes might be activated simultaneously upon induction, we analyzed the gene expression changes of gene clusters by using the microarray data. Using the public genome database, we located

Figure 6

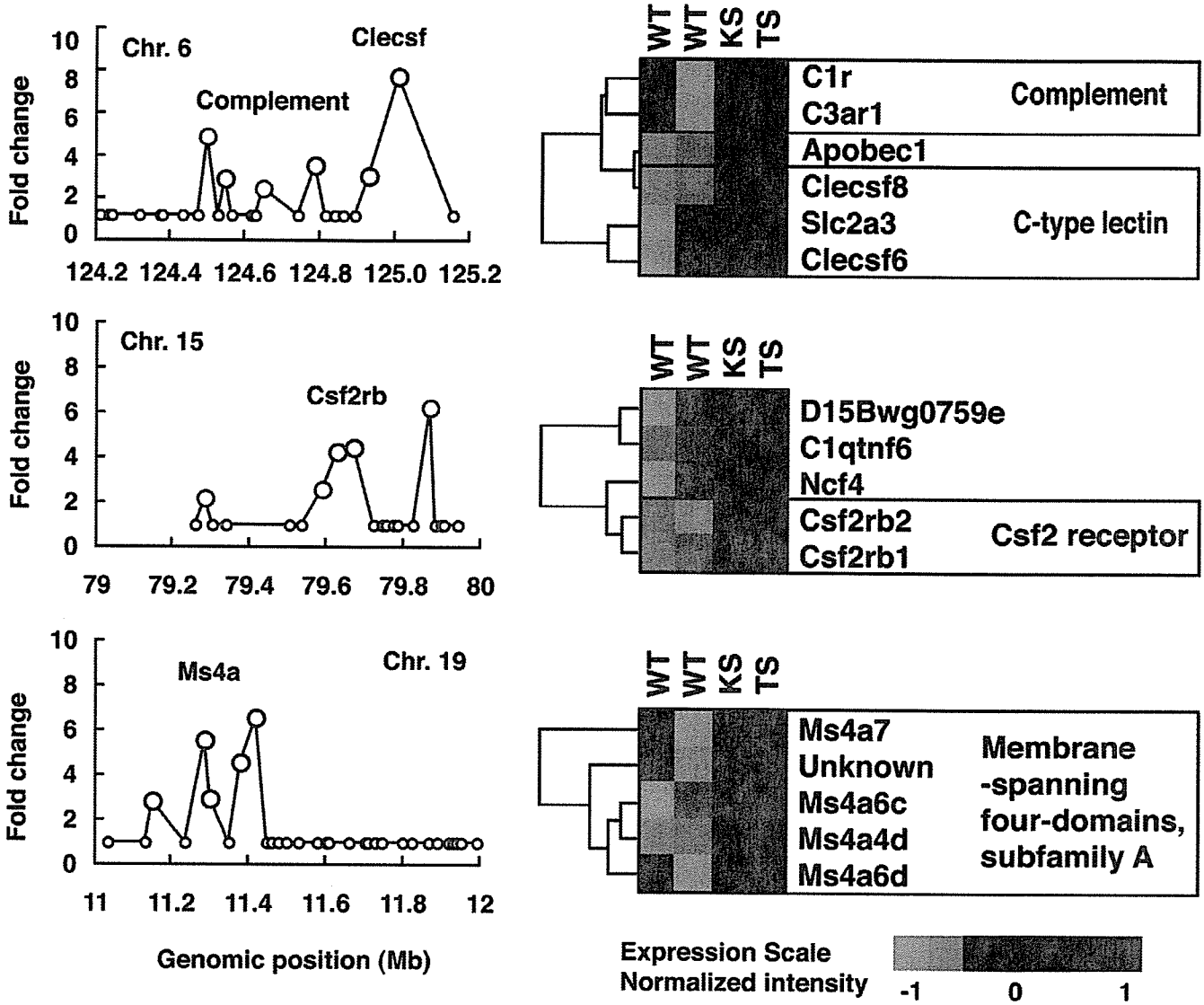

Arthritis-related gene clusters on chromosomes (Chr.) 6, 15, and 19. The peaks on the Chr. 6, 124-megabase (Mb) locus (#12) includes complement receptor genes and C-type lectin superfamily (*Clecsf*) genes, the Chr. 15, 79-Mb locus (#13) includes colony-stimulating factor 2 receptor beta (*Csf2rb*) genes, and the Chr. 19, 11-Mb locus (#14) includes membrane spanning four-domain, subfamily A (*Ms4a*) genes. Expanded views of these loci in 1-Mb scale and hierarchical clustering of the expression levels of these genes are shown.

538 of the 554 significant genes at the specific chromosomal regions. The numbers of the significant genes were plotted against each chromosome (Figure 2), giving a maximal number for chromosome 11, which included 54 genes. A second peak in gene number was found on chromosome 7, which included 43 genes. The third peak on chromosome 6 included 41 genes. Subsequently, chromosomes 1, 2, and 17 were determined to have many significant genes. The density of the significant genes was similar among all chromosomes, with the gene density of 0.022 ± 0.007 (Number of significantly changed genes/Total number of the genes in the chromosome) (shown by open circles in Figure 2). Thus, genes significantly upregulated in arthritis were broadly distributed throughout the genome.

Transcriptome mapping of arthritis-related genes

To identify individual gene clusters, significantly changed genes were mapped into the whole genome in 1-Mb scale windows. Figure 3 shows the distribution of the arthritis-related genes across the entire mouse genome; the gene clusters derived from this mapping are shown in Table 1. For convenience, peaks were numbered, and the numbers in parentheses below indicate the peaks in Figure 3. The map allocates many of the clusters of highly expressed genes to specific chromosomal regions. The maximal gene density was

mapped to the chromosome 17, 33-Mb locus (#1) and neighboring 34-Mb (#2) and 35-Mb (#3) regions, which corresponds to the *H-2* gene cluster. An expanded view of this region, shown in Figure 4, included 20 genes in a 2-Mb scale. The *H-2* gene cluster includes a number of MHC class I, MHC class II, and complement genes. Hierarchical clustering and visualization of these genes classified these significant genes into three major functionally related gene clusters, including MHC class II cluster (*H2-Dmb1*, *H2-Aa*, *H2-Ea*, *H2-DMa*, *H2-Ab1*, and *H2-Eb1*), complement cluster (*C2*, *C4*,*H2-Bf*) and MHC class I cluster (*H2-D1*,*H2-Q8*,*H2-Q10*). The expression of additional immune-related genes, including *Psmb9* (proteasome) and *Ltb* (lymphotoxin β), was also increased significantly. Another peak was on chromosome 11, 82-Mb locus (#5) and neighboring 81-Mb (#4) and 83-Mb (#6) locus, which corresponds to the *Slfn* and *Ccl* gene cluster. An expanded view of this region, shown in Figure 5, included 11 genes in a 2-Mb scale. Hierarchical clustering and visualization of these genes, including CC chemokine ligand genes (*Ccl2*, *Ccl6*, *Ccl7*, *Ccl8*, *Ccl9*, and *Ccl5*) and schlafen genes (*Slfn1*, *Slfn2, Slfn5, Slfn3*, and *Slfn4*), are shown. Moreover, chromosome 6, 68- to 70-Mb locus (#7–9) and chromosome 12, 112- and 113-Mb locus (#10,11) formed a cluster of immunoglobulin genes, kappa chain and heavy chain, respectively. High peaks were also detected at chromosome 6, 124-Mb locus (#12), which includes several genes of complement receptor and C-type lectin superfamily, and chromosome 15, 79-Mb locus (#13), which includes colony-stimulating factor 2 receptor beta (*Csf2rb*) genes, and chromosome 19, 11-Mb locus (#14), which includes membrane-spanning four-domain, subfamily A (*Ms4a*) genes. An expanded view of these loci, shown in Figure 6, included five genes in a 1-Mb scale, respectively. Chromosome 6, 124-Mb locus (#12) includes clusters of complement genes (*C1r*, *C3ar1*) and C-type lectin superfamily members (*Clecsf6*, *Clecsf8*). (*Clecsf8* mapped into the 125-Mb locus but was next to *Clecsf6*.) Chromosome 15, 79-Mb locus (#13) includes two *Csf2rb* genes (*Csf2rb1* and *Csf2rb2*). Chromosome 19, 11-Mb locus (#14) corresponds to the *Ms4a* gene cluster (*Ms4a7*,*Ms4a6c*,*Ms4a4d*,*Ms4a6d*, and an unknown gene). Although no gene family is detected in chromosome 2, 165-Mb locus (#15) and chromosome 19, 5-Mb locus (#18), chromosome 3, 146-Mb locus (#16) and chromosome 17, 17-Mb locus (#17) included gene clusters of guanylate nucleotide binding protein and formyl peptide receptor, respectively. Additional clusters of arthritis-related genes were identified, including a cluster of selectin genes on chromosome 1, 167-Mb locus (#20), Fc receptor cluster on chromosome 1, 174- and 175-Mb locus (#21), a paired-Ig-like receptor cluster on chromosome 7, 3-Mb locus (#26), serum amyloid A cluster on chromosome 7, 39-Mb locus, and the gene cluster of CC chemokine receptor on chromosome 9, 126-Mb region (#30).

Discussion

To identify genes involved in the pathogenesis of arthritis, we used two mouse models of RA. We compared the gene expression profiles between arthritic and normal joints using these models and high-density oligonucleotide arrays, in which approximately 36,000 genes and ESTs were analyzed. We analyzed whole synovial tissues instead of using specific cell types because we are interested in not only expression level changes of a gene in a cell but also cell population changes in the synovial tissues [26]. In this report, we examined two mouse models of RA on the same genetic background and with the same disease severity. These models, however, had different etiologies; one is caused by the action of HTLV-I-*tax*, whereas the other is caused by excessive IL-1 signaling. We extracted common genes that were involved in the pathogenesis of both models irrespective of etiology. We expected to identify genes involved in the effector phase of the disease, given that the molecular mechanisms of the initial phase are likely to be different between the two models. With RNA samples derived from the arthritic joints of either animal model, 1,467 clones on the array (approximately 4%) changed at least threefold. The SAM method demonstrated that, of these genes, 554 independent genes changed significantly in both models. These results suggest that a large proportion of the genes functioned in the pathogenesis of arthritis in both models. These common genes may function during the effector phase, whereas those specific to the individual models may function during the initiation phase in a manner dependent on the disease etiology. We analyzed those genes whose changes in expression levels were common to both models.

We found that several interesting genes, including *Saa3*, which encodes serum amyloid A3, were activated in these models. This gene was upregulated to the greatest extent in arthritic mice in comparison with normal mice. IL-1β induces *Saa3* expression; SAA3, in conjunction with SAA1/SAA2, the expressions of which were also elevated in our RA animal models, induce the transcription of matrix metalloproteinases (MMPs) [27]. *Mmp-3* and *Mmp-9*, two such MMPs, were also upregulated in these models. We also observed the upregulation of chemokines, such as *Cxcl5* and *Cxcl1*, which recruit neutrophils to inflammatory sites through interactions with their receptor, *Cxcr2*, which was also elevated and confirmed by northern blot analysis. *Cxcr4* may be involved in the chemotaxis of naïve and memory T cells. *Ccr1* and *Ccr2* are expressed on memory T cells, whereas *Ccr5* is expressed on Th1 cells. *Cxcl12*, the ligand for *Cxcr4*, is produced in the synovial tissues of patients with RA [28]. *Ccr6*, *Ccr1*,*Ccr2*, and *Ccr5* are specifically expressed by immature dendritic cells (DCs). *Cxcl16*, a T-cell chemoattractant, is expressed by both DCs and macrophages. *Ccl9*, *Ccl6*, and *Cxcl13* are produced by macrophages, whereas *Cxcl14* is produced by fibroblasts. In addition, proinflammatory cytokines and their cognate receptors, such as IL-1$^{\beta}$, IL-1RI, TNF-α R, IL-6Rα, IL-2R$^{\gamma}$, and IL-17R, were also significantly elevated. Thus, the augmented

expression of chemokines, cytokines, and their receptors indicates the importance of these molecules in the pathogenesis of arthritis. It should be noted, however, that the augmentation of the expression of these genes does not necessarily mean that they are actually activated in synovial tissues. The infiltrated cells to the inflammatory sites may also contribute to the expression pattern. Elevated expression of serum amyloid proteins, metalloproteinases, chemokines, and cytokines is frequently seen in the joints of patients with RA [27,29], indicating that the gene expression profiles obtained from these RA models well represent those of patients with RA. In addition, many of these genes function during the elicitation of inflammation, supporting our assumption that the genes augmented in both models may function during the effector phase.

The gene expression profiles of the well-known collagen-induced arthritis (CIA) model [30] and proteoglycan-induced arthritis (PGIA) model [31] for RA have already been reported. We compared our data set with those previously reported gene expression profiles. Approximately 60% of the genes that changed in our models also changed more than two times at the early phase of CIA. Moreover, approximately 63% of the genes corresponded to those found in PGIA at the acute phase and approximately 50% at the initiation and chronic phases. Thus, many of the genes that changed in our models also changed in other RA models, suggesting similar mechanisms function in common in those RA models.

We next mapped these arthritis-related genes into chromosomes. Working under the assumption that functionally related genes form clusters, we attempted to detect the activation of genes as a cluster, despite the fact that small individual changes were not prominent enough to be detected in our initial analysis. The most significant peak was detected at chromosome 17, 33- to 35-Mb locus (#1–3), which corresponds to the *H-2* gene cluster. Other significant peaks corresponded to chromosome 11, 81- to 83-Mb locus (#4–6), which includes members of the *Ccl* and *Slfn* families. Immunoglobulin kappa chain cluster in chromosome 6, 68- to 70-Mb locus, and heavy chain cluster in chromosome 12, 112- and 113-Mb locus were also clearly detected. Moreover, chromosome 6, 124-Mb locus, chromosome 15, 79-Mb locus, and chromosome 19, 11-Mb locus were included in those attractive gene clusters. The contribution of individual genes in these clusters was relatively small; the significance of a number of genes was recognized only after summation of genes in a specific region. These gene clusters, however, clearly contained a number of genes important in the development of arthritis. For more than two decades, the MHC gene cluster has been known to affect susceptibility to a variety of autoimmune diseases [32,33]. This region encodes the MHC class I and class II genes and other immune-related genes. MHC molecules are required for antigen recognition by lymphocytes, ultimately leading to activation and progression of immune responses. In addition, the genes encoding complement components are located within this cluster. The levels of antibodies against IgG and type II collagen were elevated in these RA models [4,7]. In these animal models, the classical pathway components of the complement system, C2, C4, encoded within this cluster (Chr. 17, 34 Mb: [#2]), and C1q, C1s, and C1r, found within other clusters, were upregulated, suggesting that immune complexes are involved in this enhancement of gene expression. The expression of Factor B, encoded by the *H2-Bf* gene within this cluster, was also augmented. Factor B is an essential component of the alternative pathway of the complement system. This pathway is also critical in K/BxN mice, another animal model for RA [34]. Although the alternative pathway typically activated by microbial surface antigens, immune complexes formed by autoreactive IgGs initiate the alternative pathway in these models to facilitate the development of arthritis.

A similar study was reported using CIA and PGIA models, identifying gene clusters in chromosomes 2, 3, 11, and 17 [35]. Their microarray chips contained a total of 9,500 known genes and EST clones, and 203 selected genes were mapped into the chromosome using a 1.5-fold differential expression threshold level. In the present study, 36,000 oligonucleotide probe sets were included in microarray chips, and 550 selected common significant genes were mapped. Interestingly, we detected the same clusters in chromosomes 2, 11, and 17 as were found in their study, suggesting that the same genes are involved in the pathogenesis of arthritis regardless of the etiology. Although they found a cluster on chromosome 3 containing 11 genes within an 8-Mb-long region, this region was not assigned as an arthritis-related gene cluster in our study, because of broad distribution of genes among cytobands. Increased expressions of MHC class I and class II genes, complement genes, and chemokine genes were already reported using microarray analysis ofsynovium from patients with RA [36] or streptococcal cell wall-induced arthritis in rats [37]. Our results in this report using mouse arthritis models are consistent with these results, suggesting that these genes are commonly involved in the pathogenesis at the elicitation phase.

The gene density peak on chromosome 11, 81- to 83-Mb locus (#4–6) includes the *Ccl* and *Slfn* genes. CCL2, CCL7, and CCL8, members of the chemokine family, recruit monocytes to sites of injury and infection. CCL2 influences innate immunity through this effect on monocytes and modulates adaptive immunity via control of Th2 polarization. An antagonist of CCL2 suppresses arthritis in the MRL-*lpr* mouse model [38]. CCL5, a T-cell and monocyte chemoattractant, plays an important role in the development of adjuvant-induced arthritis [39]. CCL6 was expressed in experimental inflammatory demyelinating disorders that promote recruitment of macrophages [40]. CCL9 recruits CD11b$^+$ DCs and promotes osteoclast differentiation and survival [41,42]. Thus, these chemokines likely play important roles in the development of arthritis. Schlafen proteins have been implicated in the regula-

tion of cell growth and T-cell development [43]. These proteins form a big family localized to a specific genomic cluster adjacent to the *Ccl* gene cluster. This region coincides with a number of autoimmune susceptibility loci, including the *Idd4*, *Eae7*, and *Orch3* loci [44]. The syntenic region of this locus on 17q of the human genome is associated with several autoimmune disorders [45]. Therefore, this genomic region on chromosome 11 is likely to be critical in the development of autoimmune arthritis.

The chromosome 6, 124-Mb (#12) locus is one of the non-MHC susceptibility loci linked to complex autoimmune diseases. The mouse 6 F2 cytoband, the syntenic rat 4q42 and human 12p13 regions, have been implicated in several inflammatory diseases, including arthritis [46-48], systemic lupus erythematosus, spontaneous diabetes, atherosclerosis, encephalomyelitis, asthma or airway hyper-responsiveness, and allergy. This locus contains complement component genes and C-type lectin superfamily genes, suggesting the possible involvement of these protein products in the development of arthritis. Chromosome 15, 79-Mb locus (#13) contains GM-CSF receptor, *Csf2rb1*, and *Csf2rb2*. It is known that GM-CSF plays an important role in the effector phase of arthritis [49]. *Ms4a* family molecules, CD20 (*Ms4a1*), and high-affinity IgE receptor β chain (FcΣ RIb; *Ms4a2*) tended to be upregulated in these animals, but these genes were not significantly altered in this study. Although the upregulation of *Ms4a7*, *Ms4a4d*, *Ms4a6d*, and *Ms4a6c* expression in chromosome 19, 11-Mb locus (#14) was also observed in these models of RA, the roles of these molecules in the development of arthritis are not yet known [50].

We succeeded in identifying several arthritis-related genes by transcriptome mapping, but we might have failed to detect some potentially important genes. Because we analyzed mRNA preparations from whole joints, but not from a single species of cell, we could not detect the change of gene expression in a single species of cell when the content of this single species of cell was low in the whole joint. Furthermore, we could not detect the MMP gene cluster consisting of MMP-1a, MMP-1b, MMP-3, and MMP-13 on chromosome 9, which were suggested to be involved in the pathogenesis [51]. In this case, we demonstrated upregulation of MMP-3 and MMP-9 in both HTLV-I-Tg and IL-1Ra-KO mice. However, MMP-8 and MMP-13 expressions were increased more than three times in IL-1Ra-KO mice, but not in HTLV-I-Tg mice, excluding the *MMP-8* and *MMP-13* genes from significantly activated genes in this analysis. Unfortunately, MMP-1a and MMP-1b were not mounted on the GeneChip we used (Murine Genome U74v2 Set). Nonetheless, the present data are important for understanding the transcriptome change as a whole, reflecting the gene expression levels not only in a single cell but also in the cell population in the joints during arthritis.

Conclusion

We have performed a comprehensive transcriptome analysis of two etiologically different RA models by using microarrays and identified many genes that were commonly activated in both models. Because the initial mechanism of the pathogenesis should be different between two models, these genes are likely to function during the effector phase of the disease. Moreover, by mapping genes with marginal expression changes into chromosomes, we succeeded in detecting several gene clusters that may be involved in the pathogenesis of arthritis. A similar approach, using microarrays, will likely be useful in detecting genes related to multiple disease processes.

Competing interests

The authors declare that they have no competing interests.

Authors' contributions

NF, SS, and YI participated in the design of the study. SS prepared the RNA samples and carried out northern blot hybridization with NF. NF carried out the analysis of the microarray data, developed the transcriptome mapping analysis method, and drafted this manuscript as a part of his doctoral thesis. YI planned, designed, and organized the study and finalized the manuscript. All authors read and approved the final manuscript.

Additional files

The following Additional files are available online:

Additional File 1

An Excel file containing a table that lists the first 1,467 selected genes, the expression of which changed more than three times in one of the mouse models.
See http://www.biomedcentral.com/content/supplementary/ar1985-S1.xls

Additional File 2

An Excel file containing a table that lists five hundred fifty-four non-redundant genes, the expression of which significantly changed in both models.
See http://www.biomedcentral.com/content/supplementary/ar1985-S2.xls

Acknowledgements

We thank Drs. Michiyasu Takeyama and Reiko Sasada at Discovery Research Laboratories II, Takeda Chemical Industries Ltd., for kind analysis with microarrays, and Dr. Sumio Sugano, Human Genome Center, Institute of Medical Science, University of Tokyo, for kindly providing a mouse spleen cDNA library. We also thank all of the members of the laboratory for their excellent animal care. This research was supported by grants from the Ministry of Education, Science, Sport and Culture of

Japan and the Ministry of Health and Welfare of Japan and a fellowship from the Japan Society for the Promotion of Science.

References

1. Firestein GS, Zvaifler NJ: *Rheumatoid Arthritis: A Disease of Disordered Immunity* New York: Raven Press; 1992.
2. Iwakura Y: **Roles of IL-1 in the development of rheumatoid arthritis: consideration from mouse models.** *Cytokine Growth Factor Rev* 2002, **13**:341-355.
3. Iwakura Y, Tosu M, Yoshida E, Takiguchi M, Sato K, Kitajima I, Nishioka K, Yamamoto K, Takeda T, Hatanaka M, *et al.*: **Induction of inflammatory arthropathy resembling rheumatoid arthritis in mice transgenic for HTLV-I.** *Science* 1991, **253**:1026-1028.
4. Horai R, Saijo S, Tanioka H, Nakae S, Sudo K, Okahara A, Ikuse T, Asano M, Iwakura Y: **Development of chronic inflammatory arthropathy resembling rheumatoid arthritis in interleukin 1 receptor antagonist-deficient mice.** *J Exp Med* 2000, **191**:313-320.
5. Yoshida M: **HTLV-I tax: regulation of gene expression and disease.** *Trends Microbiol* 1993, **1**:131-135.
6. Sugamura K, Hinuma Y: *Human Retroviruses: HTLV-I and HTLV-II Volume 2.* New York: Plenum Press; 1993.
7. Iwakura Y, Saijo S, Kioka Y, Nakayama-Yamada J, Itagaki K, Tosu M, Asano M, Kanai Y, Kakimoto K: **Autoimmunity induction by human T cell leukemia virus type 1 in transgenic mice that develop chronic inflammatory arthropathy resembling rheumatoid arthritis in humans.** *J Immunol* 1995, **155**:1588-1598.
8. Horai R, Nakajima A, Habiro K, Kotani M, Nakae S, Matsuki T, Nambu A, Saijo S, Kotaki H, Sudo K, *et al.*: **TNF-alpha is crucial for the development of autoimmune arthritis in IL-1 receptor antagonist-deficient mice.** *J Clin Invest* 2004, **114**:1603-1611.
9. Motokawa S, Hasunuma T, Tajima K, Krieg AM, Ito S, Iwasaki K, Nishioka K: **High prevalence of arthropathy in HTLV-I carriers on a Japanese island.** *Ann Rheum Dis* 1996, **55**:193-195.
10. Eguchi K, Origuchi T, Takashima H, Iwata K, Katamine S, Nagataki S: **High seroprevalence of anti-HTLV-I antibody in rheumatoid arthritis.** *Arthritis Rheum* 1996, **39**:463-466.
11. Perrier S, Coussediere C, Dubost JJ, Albuisson E, Sauvezie B: **IL-1 receptor antagonist (IL-1RA) gene polymorphism in Sjogren's syndrome and rheumatoid arthritis.** *Clin Immunol Immunopathol* 1998, **87**:309-313.
12. Cantagrel A, Navaux F, Loubet-Lescoulie P, Nourhashemi F, Enault G, Abbal M, Constantin A, Laroche M, Mazieres B: **Interleukin-1beta, interleukin-1 receptor antagonist, interleukin-4, and interleukin-10 gene polymorphisms: relationship to occurrence and severity of rheumatoid arthritis.** *Arthritis Rheum* 1999, **42**:1093-1100.
13. Caron H, van Schaik B, van der Mee M, Baas F, Riggins G, van Sluis P, Hermus MC, van Asperen R, Boon K, Voute PA, *et al.*: **The human transcriptome map: clustering of highly expressed genes in chromosomal domains.** *Science* 2001, **291**:1289-1292.
14. Lercher MJ, Urrutia AO, Hurst LD: **Clustering of housekeeping genes provides a unified model of gene order in the human genome.** *Nat Genet* 2002, **31**:180-183.
15. Cremer T, Cremer C: **Chromosome territories, nuclear architecture and gene regulation in mammalian cells.** *Nat Rev Genet* 2001, **2**:292-301.
16. de Laat W, Grosveld F: **Spatial organization of gene expression: the active chromatin hub.** *Chromosome Res* 2003, **11**:447-459.
17. Tusher VG, Tibshirani R, Chu G: **Significance analysis of microarrays applied to the ionizing radiation response.** *Proc Natl Acad Sci U S A* 2001, **98**:5116-5121.
18. **National Center for Biotechnology Information** [http://www.ncbi.nlm.nih.gov/]
19. **SOURCE** [http://source.stanford.edu]
20. **The Bioinformatics Analytical Toolkit** [http://www.mouse-genome.bcm.tmc.edu]
21. **Cluster Analysis and Visualization** [http://rana.lbl.gov/EisenSoftware.htm]
22. Eisen MB, Spellman PT, Brown PO, Botstein D: **Cluster analysis and display of genome-wide expression patterns.** *Proc Natl Acad Sci U S A* 1998, **95**:14863-14868.
23. Chapuy-Regaud S, Nogueira L, Clavel C, Sebbag M, Vincent C, Serre G: **IgG subclass distribution of the rheumatoid arthritis-specific autoantibodies to citrullinated fibrin.** *Clin Exp Immunol* 2005, **139**:542-550.
24. Ainola MM, Mandelin JA, Liljestrom MP, Li TF, Hukkanen MV, Konttinen YT: **Pannus invasion and cartilage degradation in rheumatoid arthritis: involvement of MMP-3 and interleukin-1beta.** *Clin Exp Rheumatol* 2005, **23**:644-650.
25. Hurst LD, Pal C, Lercher MJ: **The evolutionary dynamics of eukaryotic gene order.** *Nat Rev Genet* 2004, **5**:299-310.
26. Gregersen PK, Brehrens TW: **Fine mapping the phenotype in autoimmune disease: the promise and pitfalls of DNA microarray technologies.** *Genes Immun* 2003, **4**:175-176.
27. Vallon R, Freuler F, Desta-Tsedu N, Robeva A, Dawson J, Wenner P, Engelhardt P, Boes L, Schnyder J, Tschopp C, *et al.*: **Serum amyloid A (apoSAA) expression is up-regulated in rheumatoid arthritis and induces transcription of matrix metalloproteinases.** *J Immunol* 2001, **166**:2801-2807.
28. Nanki T, Hayashida K, El-Gabalawy HS, Suson S, Shi K, Girschick HJ, Yavuz S, Lipsky PE: **Stromal cell-derived factor-1-CXC chemokine receptor 4 interactions play a central role in CD4+T cell accumulation in rheumatoid arthritis synovium.** *J Immunol* 2000, **165**:6590-6598.
29. Firestein GS: **Evolving concepts of rheumatoid arthritis.** *Nature* 2003, **423**:356-361.
30. Thornton S, Sowders D, Aronow B, Witte DP, Brunner HI, Giannini EH, Hirsch R: **DNA microarray analysis reveals novel gene expression profiles in collagen-induced arthritis.** *Clin Immunol* 2002, **105**:155-168.
31. Adarichev VA, Vermes C, Hanyecz A, Mikecz K, Bremer EG, Glant TT: **Gene expression profiling in murine autoimmune arthritis during the initiation and progression of joint inflammation.** *Arthritis Res Ther* 2005, **7**:R196-207.
32. Deighton CM, Walker DJ, Griffiths ID, Roberts DF: **The contribution of HLA to rheumatoid arthritis.** *Clin Genet* 1989, **36**:178-182.
33. Marrack P, Kappler J, Kotzin BL: **Autoimmune disease: why and where it occurs.** *Nat Med* 2001, **7**:899-905.
34. Ji H, Ohmura K, Mahmood U, Lee DM, Hofhuis FM, Boackle SA, Takahashi K, Holers VM, Walport M, Gerard C, *et al.*: **Arthritis critically dependent on innate immune system players.** *Immunity* 2002, **16**:157-168.
35. Firneisz G, Zehavi I, Vermes C, Hanyecz A, Frieman JA, Glant TT: **Identification and quantification of disease-related gene clusters.** *Bioinformatics* 2003, **19**:1781-1786.
36. van der Pouw Kraan TC, van Gaalen FA, Huizinga TW, Pieterman E, Breedveld FC, Verweij CL: **Discovery of distinctive gene expression profiles in rheumatoid synovium using cDNA microarray technology: evidence for the existence of multiple pathways of tissue destruction and repair.** *Genes Immun* 2003, **4**:187-196.
37. Rioja I, Clayton CL, Graham SJ, Life PF, Dickson MC: **Gene expression profiles in the rat streptococcal cell wall-induced arthritis model identified using microarray analysis.** *Arthritis Res Ther* 2005, **7**:R101-117.
38. Gong JH, Ratkay LG, Waterfield JD, Clark-Lewis I: **An antagonist of monocyte chemoattractant protein 1 (MCP-1) inhibits arthritis in the MRL-lpr mouse model.** *J Exp Med* 1997, **186**:131-137.
39. Barnes DA, Tse J, Kaufhold M, Owen M, Hesselgesser J, Strieter R, Horuk R, Perez HD: **Polyclonal antibody directed against human RANTES ameliorates disease in the Lewis rat adjuvant-induced arthritis model.** *J Clin Invest* 1998, **101**:2910-2919.
40. Asensio VC, Lassmann S, Pagenstecher A, Steffensen SC, Henriksen SJ, Campbell IL: **C10 is a novel chemokine expressed in experimental inflammatory demyelinating disorders that promotes recruitment of macrophages to the central nervous system.** *Am J Pathol* 1999, **154**:1181-1191.
41. Zhao X, Sato A, Dela Cruz CS, Linehan M, Luegering A, Kucharzik T, Shirakawa AK, Marquez G, Farber JM, Williams I, *et al.*: **CCL9 is secreted by the follicle-associated epithelium and recruits dome region Peyer's patch CD11b+ dendritic cells.** *J Immunol* 2003, **171**:2797-2803.
42. Okamatsu Y, Kim D, Battaglino R, Sasaki H, Spate U, Stashenko P: **MIP-1 gamma promotes receptor-activator-of-NF-kappa-B-ligand-induced osteoclast formation and survival.** *J Immunol* 2004, **173**:2084-2090.

43. Schwarz DA, Katayama CD, Hedrick SM: **Schlafen, a new family of growth regulatory genes that affect thymocyte development.** *Immunity* 1998, **9**:657-668.
44. Griffiths MM, Encinas JA, Remmers EF, Kuchroo VK, Wilder RL: **Mapping autoimmunity genes.** *Curr Opin Immunol* 1999, **11**:689-700.
45. Wandstrat A, Wakeland E: **The genetics of complex autoimmune diseases: non-MHC susceptibility genes.** *Nat Immunol* 2001, **2**:802-809.
46. McIndoe RA, Bohlman B, Chi E, Schuster E, Lindhardt M, Hood L: **Localization of non-Mhc collagen-induced arthritis susceptibility loci in DBA/1j mice.** *Proc Natl Acad Sci U S A* 1999, **96**:2210-2214.
47. Lorentzen JC, Glaser A, Jacobsson L, Galli J, Fakhrai-rad H, Klareskog L, Luthman H: **Identification of rat susceptibility loci for adjuvant-oil-induced arthritis.** *Proc Natl Acad Sci U S A* 1998, **95**:6383-6387.
48. Cornelis F, Faure S, Martinez M, Prud'homme JF, Fritz P, Dib C, Alves H, Barrera P, de Vries N, Balsa A, *et al.*: **New susceptibility locus for rheumatoid arthritis suggested by a genome-wide linkage study.** *Proc Natl Acad Sci U S A* 1998, **95**:10746-10750.
49. Cook AD, Braine EL, Campbell IK, Rich MJ, Hamilton JA: **Blockade of collagen-induced arthritis post-onset by antibody to granulocyte-macrophage colony-stimulating factor (GM-CSF): requirement for GM-CSF in the effector phase of disease.** *Arthritis Res* 2001, **3**:293-298.
50. Liang Y, Tedder TF: **Identification of a CD20-, FcepsilonRIbeta-, and HTm4-related gene family: sixteen new MS4A family members expressed in human and mouse.** *Genomics* 2001, **72**:119-127.
51. Dorr S, Lechtenbohmer N, Rau R, Herborn G, Wagner U, Muller-Myhsok B, Hansmann I, Keyszer G: **Association of a specific haplotype across the genes MMP1 and MMP3 with radiographic joint destruction in rheumatoid arthritis.** *Arthritis Res Ther* 2004, **6**:R199-207.

Dok-1 and Dok-2 are negative regulators of lipopolysaccharide-induced signaling

Hisaaki Shinohara,[1,2] Akane Inoue,[1] Noriko Toyama-Sorimachi,[3] Yoshinori Nagai,[4] Tomoharu Yasuda,[1] Hiromi Suzuki,[5] Reiko Horai,[6] Yoichiro Iwakura,[6] Tadashi Yamamoto,[5] Hajime Karasuyama,[3] Kensuke Miyake,[4] and Yuji Yamanashi[1,2]

[1]Department of Cell Regulation, Medical Research Institute, [2]School of Biomedical Science, and [3]Department of Immune Regulation, Graduate School, Tokyo Medical and Dental University, Tokyo 113-8510, Japan
[4]Division of Infectious Genetics, [5]Department of Oncology, and [6]Center for Experimental Medicine, Institute of Medical Science, University of Tokyo, Tokyo 108-8639, Japan

Endotoxin, a bacterial lipopolysaccharide (LPS), causes fatal septic shock via Toll-like receptor (TLR)4 on effector cells of innate immunity like macrophages, where it activates nuclear factor κB (NF-κB) and mitogen-activated protein (MAP) kinases to induce proinflammatory cytokines such as tumor necrosis factor (TNF)-α. Dok-1 and Dok-2 are adaptor proteins that negatively regulate Ras–Erk signaling downstream of protein tyrosine kinases (PTKs). Here, we demonstrate that LPS rapidly induced the tyrosine phosphorylation and adaptor function of these proteins. The stimulation with LPS of macrophages from mice lacking Dok-1 or Dok-2 induced elevated Erk activation, but not the other MAP kinases or NF-κB, resulting in hyperproduction of TNF-α and nitric oxide. Furthermore, the mutant mice showed hyperproduction of TNF-α and hypersensitivity to LPS. However, macrophages from these mutant mice reacted normally to other pathogenic molecules, CpG oligodeoxynucleotides, poly(I:C) ribonucleotides, or Pam_3CSK_4 lipopeptide, which activated cognate TLRs but induced no tyrosine phosphorylation of Dok-1 or Dok-2. Forced expression of either adaptor, but not a mutant having a Tyr/Phe substitution, in macrophages inhibited LPS-induced Erk activation and TNF-α production. Thus, Dok-1 and Dok-2 are essential negative regulators downstream of TLR4, implying a novel PTK-dependent pathway in innate immunity.

CORRESPONDENCE
Yuji Yamanashi:
yamanashi.creg@mri.tmd.ac.jp

The innate immune response to microbial pathogens begins when pathogen-associated molecular patterns (PAMPs) meet their cognate receptors on effector cells. PAMPs are conserved motifs on pathogens that are usually not found in higher eukaryotes and include LPS, a bacterial cell wall component and the most potent stimulator in innate immunity (1). Toll-like receptors (TLRs) recognize PAMPs, and LPS stimulates the TLR4–MD-2 receptor complex, which then triggers intracellular signaling cascades (TLR4 signaling) including the activation of NF-κB and three types of mitogen-activated protein (MAP) kinases: Erk, JNK, and p38 (2, 3). These signaling molecules play indispensable roles in inducing TNF-α, a key proinflammatory cytokine for innate immunity (4). Recent studies have revealed that another LPS receptor, CD14, facilitates the binding of LPS to the TLR4–MD-2 complex and consequent intracellular signaling (5). In addition, TLR-mediated signaling depends upon adaptor molecules such as MyD88 and Toll/IL-1 receptor domain–containing adaptor-inducing IFN-β (TRIF) and is often classified into a MyD88- or TRIF-dependent pathway. In fact, TLR4 triggers both pathways, and macrophages from mice lacking these adaptors are defective in proinflammatory responses to LPS (6).

Although the innate immune response is essential for controlling the growth of pathogenic microbes, negative regulation is also critical because excessive and unleashed responses can cause inflammatory diseases such as septic shock or chronic inflammation (4, 7–10). A Toll IL-1 receptor family protein ST2 was recently reported as an inducible negative regulator of the MyD88-dependent pathway (7). Indeed, mice lacking ST2 failed to develop endotoxin tolerance a few days after primary administra-

H. Shinohara's present address is Laboratory for Lymphocyte Differentiation, RIKEN Research Center for Allergy and Immunology, Kanagawa 230-0045, Japan.

The online version of this article contains supplemental material.

JEM © The Rockefeller University Press $8.00
Vol. 201, No. 3, February 7, 2005 333–339 www.jem.org/cgi/doi/10.1084/jem.20041817

tion of a sublethal dose of LPS. However, due to the lag period for its induction, ST2 appeared irrelevant to primary endotoxin shock, a septic shock rapidly induced by LPS. Gene targeting studies further revealed that IL-1 receptor–associated kinase (IRAK)-M and suppressor of cytokine signaling 1 are inducible negative regulators of LPS responses (8–10). Despite these findings, very little is known about constitutively expressed negative regulator(s) of TLR4 signaling, which could work instantaneously upon LPS treatment of macrophages to control the early phase of the signaling and oppose endotoxin shock.

Dok-1 was originally identified as a major substrate of many protein tyrosine kinases (PTKs; references 11–13). When tyrosine phosphorylated, Dok-1 and its closest homologue Dok-2 work as adaptor proteins and recruit multiple SH2-containing molecules such as p120 rasGAP and Nck. These adaptors are preferentially expressed in hematopoietic cells and share structural similarities characterized by NH_2-terminal PH and PTB domains, followed by COOH-terminal SH2 target motifs (11). Experiments with mice lacking Dok-1 or Dok-2 demonstrated an indispensable role in the negative regulation of Erk downstream of PTKs in various hematopoietic cells (14–16). However, mice lacking either adaptor did not show overt defects in hematopoiesis. Although the biological significance of PTKs in TLR4 signaling is controversial, LPS activates cytoplasmic PTKs including Lyn, which is essential for the phosphorylation of Dok-1 upon B cell receptor signaling (15, 17). Here, we have studied the role of Dok-1 and Dok-2 and demonstrate that these adaptors are constitutively expressed negative regulators of TLR4 signaling.

RESULTS AND DISCUSSION

Dok-1 and Dok-2 are negative regulators of TNF-α and nitric oxide (NO) production upon LPS treatment of macrophages

To understand the role of Dok-1 and Dok-2 in TLR4 signaling, we first examined the production of two major signal mediators of innate immunity, TNF-α and NO, upon LPS treatment of macrophages from mice lacking Dok-1 or Dok-2. The peritoneal resident and BM-derived macrophages from either of the mutant mice showed a larger population of TNF-α–producing cells and greater NO production than the wild-type cells, respectively (Fig. 1, A and B). However, both mutant macrophages expressed normal levels of LPS receptors, TLR4–MD-2, and CD14, indicating that loss of Dok-1 or Dok-2 does not cause down-regulation of these receptors (Fig. S1, available at http://www.jem.org/cgi/content/full/jem.20041817/DC1). Thus, Dok-1 and Dok-2 are indispensable negative regulators of TNF-α and NO production downstream of TLR4.

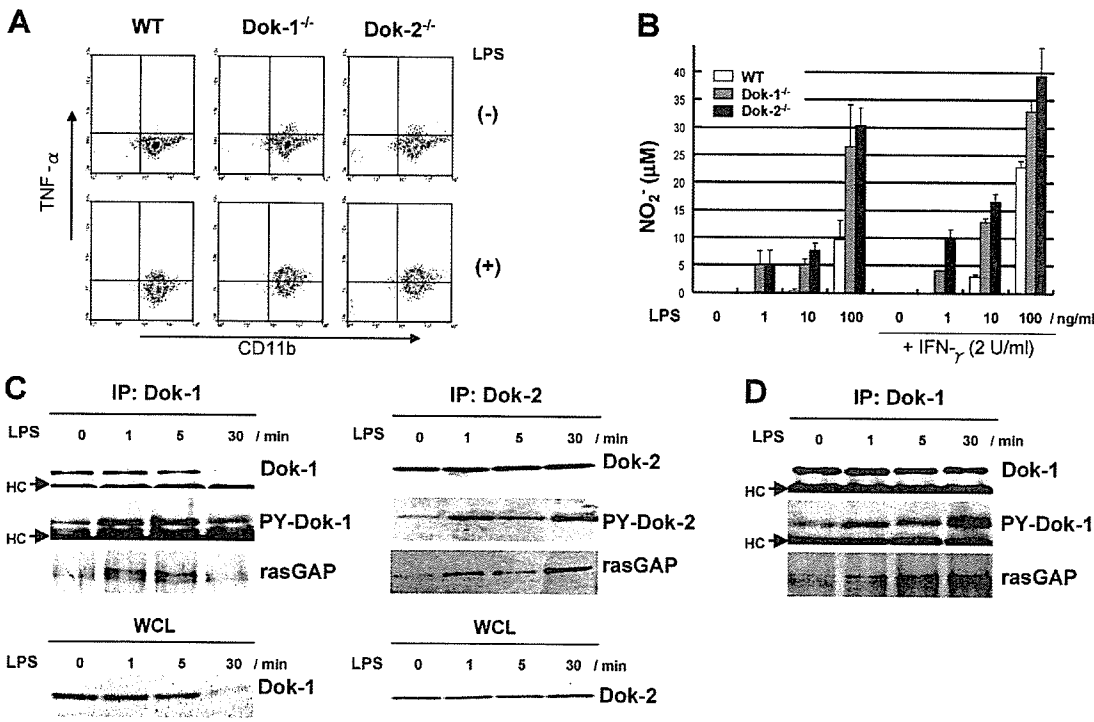

Figure 1. Dok-1 and Dok-2 are adaptors essential to the negative regulation of LPS responses. (A) Peritoneal resident macrophages from mice were treated with (+) or without (−) LPS, and then intracellular TNF-α production of $CD11b^+$ cells was examined with flow cytometry. (B) BM-derived macrophages were cultured in the indicated concentration of LPS and IFN-γ, and then NO production was evaluated. SD is from sextuplicate experiments. (C) Dok-1 or Dok2 immunoprecipitates (IP) or whole cell lysates (WCL) were subjected to immunoblotting for Dok-1, Dok-2, phosphotyrosine (PY-Dok-1 or PY-Dok-2), or p120 rasGAP upon LPS treatment of peritoneal macrophages for the indicated period. Position of immunoglobulin heavy chain (HC) is indicated. (D) Dok-1 immunoprecipitates were adjusted to contain the same levels of Dok-1 in quantity and examined as in C.

Dok-1 and Dok-2 are essential adaptors in the negative regulation of Erk upon LPS treatment

To address the molecular mechanisms of the Dok-1– and Dok-2–mediated negative regulation of LPS-evoked responses, we examined the tyrosine phosphorylation and adaptor function in peritoneal macrophages. Antiphosphotyrosine immunoblot and coimmunoprecipitation analyses revealed that the Dok family proteins were indeed tyrosine phosphorylated as early as 1 min after LPS treatment and coimmunoprecipitated with p120 rasGAP (Fig. 1 C). Interestingly, Dok-1, but not Dok-2, decreased in quantity at least 30 min after the stimulation, indicating that the biochemical responses of these proteins differ. However, when immunoprecipitated Dok-1 was adjusted to the same quantity at each time point, its tyrosine phosphorylation and binding to rasGAP was obvious even 30 min after the stimulation with LPS (Fig. 1 D). These results indicate that Dok-1 and Dok-2 are adaptors involved in LPS-evoked signaling, which activates PTK(s) to phosphorylate them, and also suggest that these adaptors negatively regulate Erk upon TLR4 signaling, like in many other signaling situations downstream of PTKs. Thus, the activation of Erk as well as JNK and p38 MAP kinase was evaluated upon LPS treatment of BM-derived macrophages from mice lacking Dok-1 or Dok-2. Although JNK and p38 MAP kinase activation was normal in those macrophages, the activation of Erk was remarkably enhanced and sustained (Fig. 2 A). In addition, the phosphorylation and degradation of IκB-α as well as the activation of

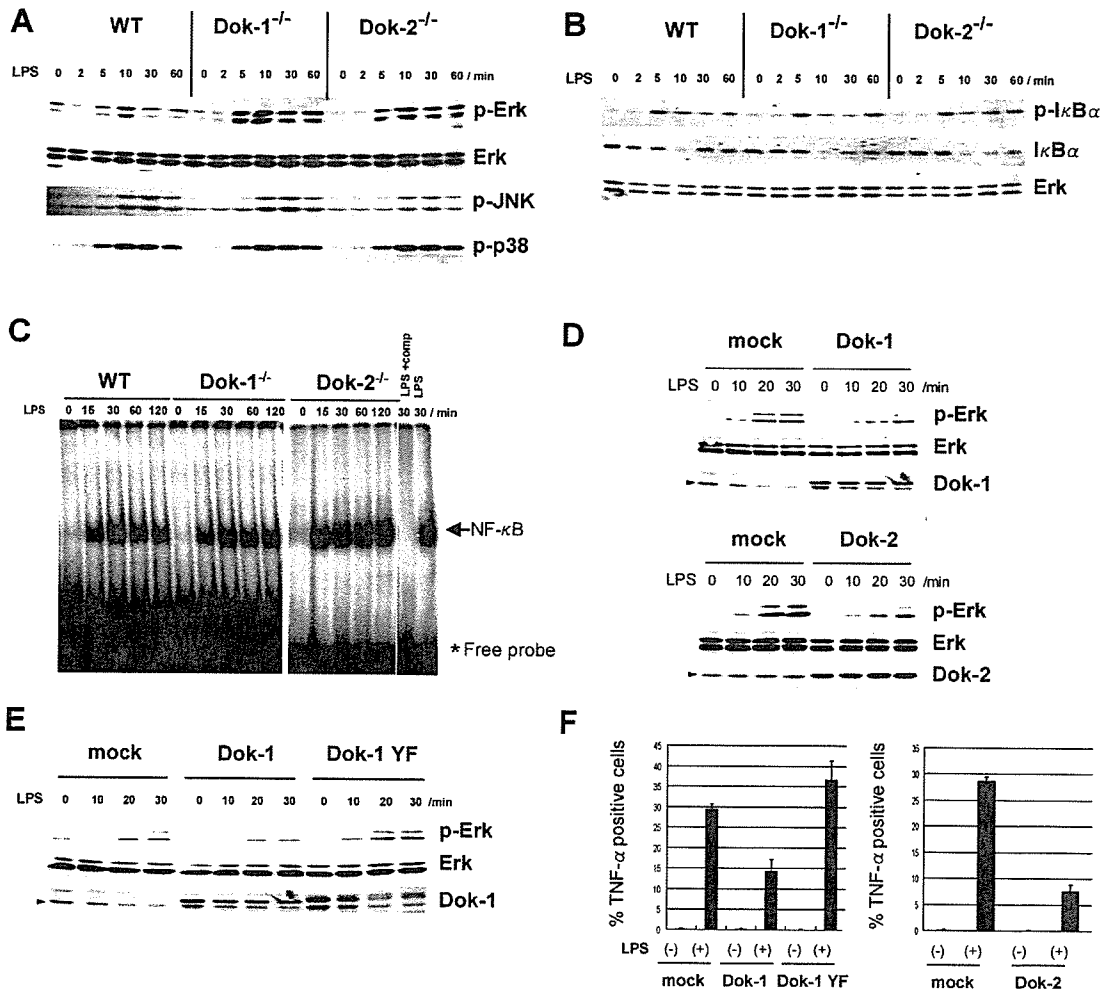

Figure 2. Dok-1 and Dok-2 are negative regulators of Erk upon TLR4 signaling. (A) Total Erk, activated Erk (p-Erk), JNK (p-JNK), or p38 MAP kinase (p-p38) was examined with immunoblotting upon LPS treatment of BM-derived macrophages from mice. (B) NF-κB activation was assessed by immunoblotting for IκBα or its phosphorylation (p-IκBα) upon LPS treatment of macrophages in A. Control immunoblotting for Erk was performed. (C) NF-κB activity was examined by gel mobility shift assay upon LPS treatment of peritoneal macrophages. Positions of the NF-κB complex and the free probes are indicated. The specificity was determined by adding excess amounts of unlabeled competitor of the probe (LPS + comp) or not (LPS) to nuclear extracts of wild-type macrophages. (D) Activated Erk (p-Erk), total Erk, Dok-1, or Dok-2 was examined with immunoblotting upon LPS treatment of RAW 264.7 cells (mock) or those expressing exogenous Dok-1 (top) or Dok-2 (bottom). An arrowhead indicates the position of endogenous Dok-1 or Dok-2. (E) RAW 264.7 cells (mock) or those expressing exogenous Dok-1 or a Dok-1 mutant (Dok-1 YF) were examined as in D. (F) RAW 264.7 cells (mock) or those expressing exogenous Dok-1, Dok-1 YF, or Dok-2 were cultured in the presence (+) or absence (−) of LPS, and then the percentage of intracellular TNF-α$^+$ cells was determined with flow cytometry. SD is from triplicate experiments.

NF-κB were unaffected in macrophages regardless of the mutations (Fig. 2, B and C). Together, our findings demonstrate that Dok-1 and Dok-2 are essential adaptors in the negative regulation of Erk, but not JNK, p38 MAP kinase, and NF-κB, upon TLR4 signaling. Moreover, that the expression levels of Dok-1 and Dok-2 were unchanged at least early on and the phosphorylation was very rapid upon LPS treatment indicates that both adaptors are on standby before the onset of the signaling to be rapidly activated (Fig. 1 C).

Forced expression of Dok-1 or Dok-2 inhibits LPS-induced Erk activation and TNF-α production

To confirm that Dok-1 and Dok-2 are negative regulators of Erk and TNF-α responses to LPS, we examined if forced expression in macrophages of either adaptor suffices to inhibit those responses. The control RAW 264.7 macrophages displayed an intact Erk activation, TNF-α production, and Dok-1 down-regulation upon LPS treatment (Fig. 2, D–F). However, forced expression of flag-tagged Dok-1 or Dok-2 clearly inhibited the Erk and TNF-α responses to LPS, indicating that Dok-1 and Dok-2 are potent negative regulators of the signaling. Note that the flag-tagged Dok-1, but not Dok-2, was down-regulated like the endogenous Dok-1. Recently, we identified Tyr-336 and Tyr-340 as essential residues for Dok-1 to inhibit the Ras–Erk pathway downstream of Lyn (18). Consistently, forced expression of a flag-tagged Dok-1 mutant having a Tyr/Phe substitution at these residues (Dok-1 YF) resulted in a loss of inhibitory effects on the LPS-evoked responses (Fig. 2, E and F). These results strongly suggest that tyrosine phosphorylation of Dok-1 and probably Dok-2 is essential for the inhibitory effects downstream of TLR4.

Although little is known about the regulation of Erk downstream of LPS, it was reported that a MAP kinase kinase kinase, Tpl2/Cot, is required for the LPS-mediated activation of Erk in macrophages (19). The authors showed that loss of Tpl2 specifically blocks the activation of Erk among MAP kinases and NF-κB and that inhibition of MEK, and thereby inhibition of Erk, suppressed TNF-α production upon LPS signaling. Moreover, it was suggested that not only LPS but also Tpl2 requires the Ras pathway to activate Erk (20, 21). Therefore, Ras appears to be an essential element for the activation of Erk downstream of TLR4. Given that the Dok-1 YF mutant lacking residues essential for the inhibition of Ras had no inhibitory effect upon TLR4 signaling (Fig. 2, E and F), the negative signaling of Dok-1 against Erk may intersect the Tpl2-mediated positive signaling in the Ras pathway downstream of TLR4. Further studies are required to understand molecular mechanisms of the Dok-1 and Dok-2 function in the TLR4 pathway, including the negative regulation of TNF-α production and interaction with their regulators and effectors.

Dok-1 and Dok-2 are irrelevant to TLR9, TLR3, or TLR2 signaling

To delineate the Dok-1 and Dok-2 function in TLR-mediated signaling, we examined their role upon the stimulation of macrophages with CpG oligodeoxynucleotide (ODN) and poly(I:C), which mimic microbial nucleotides and induce MyD88-dependent and TRIF-dependent pathways through TLR9 and TLR3, respectively. Interestingly, both nucleotides induced normal levels of Erk, JNK, and p38 MAP kinase activation as well as TNF-α production regardless of Dok-1 or Dok-2 mutation, indicating that both adaptors are dispensable to the signaling downstream of these TLRs (Fig. 3, A and B, and Fig. S2, available at http://www.jem.org/cgi/content/full/jem.20041817/DC1). Because TLR3 and TLR9 are thought to be intracellular receptors, whereas

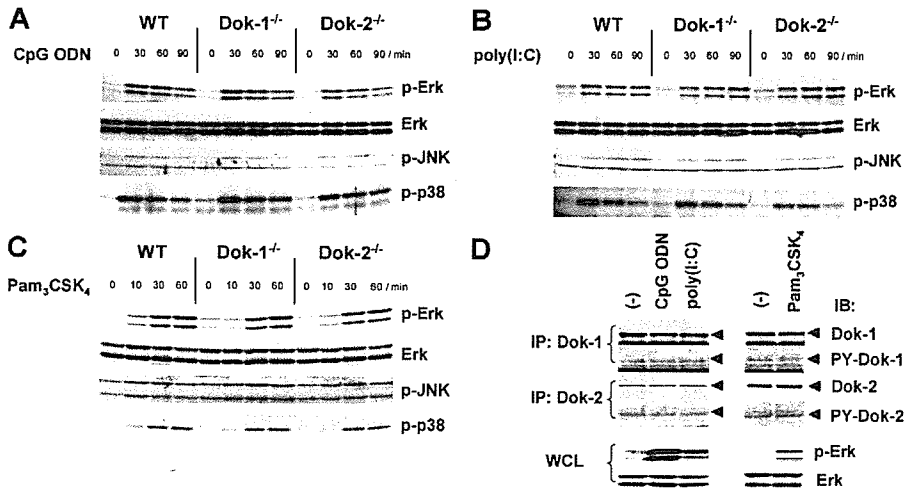

Figure 3. Dok-1 and Dok-2 are irrelevant to TLR9, TLR3, or TLR2 signaling. (A–C) Activation of each MAP kinase was examined as in Fig. 2 A upon CpG ODN, poly(I:C), or Pam_3CSK_4 treatment of BM-derived macrophages from mice. (D) Dok-1 or Dok-2 immunoprecipitates (IP) were subjected to immunoblotting (IB) for Dok-1, Dok-2, or phosphotyrosine (PY-Dok-1 or PY-Dok-2) upon CpG ODN, poly(I:C), or Pam_3CSK_4 treatment of wild-type peritoneal macrophages for 30 min. Whole cell lysates (WCL) from these macrophages were subjected to immunoblotting for activated Erk (p-Erk) or total Erk as controls.

TLR4 is present on the cell surface (22), we further examined the role of Dok-1 and Dok-2 upon the stimulation of macrophages with Pam_3CSK_4, which is an analogue of bacterial outer membrane lipoproteins and activates the MyD88-dependent pathway through a cell surface receptor, TLR2. However, Pam_3CSK_4 induced normal levels of MAP kinase activation and TNF-α production regardless of Dok-1 or Dok-2 mutation, indicating that both adaptors are dispensable to TLR2 signaling (Fig. 3 C and Fig. S2). Consistently, CpG-ODN, poly(I:C), or Pam_3CSK_4 treatment did not induce tyrosine phosphorylation of Dok-1 and Dok-2 or down-regulation of Dok-1, indicating that these adaptors are irrelevant to TLR9, TLR3, or TLR2 signaling (Fig. 3 D). Together, Dok-1 and Dok-2 are essential adaptors for the negative regulation of Erk specifically upon LPS treatment, likely because LPS, but not CpG ODN, poly(I:C), or Pam_3CSK_4, induces their tyrosine phosphorylation.

Mice lacking Dok-1 or Dok-2 are hypersensitive to LPS

Our in vitro and ex vivo findings suggest that mice lacking Dok-1 or Dok-2 are hypersensitive to LPS; therefore, we examined TNF-α production upon i.p. administration of LPS to such mutant mice. Because overproduction of TNF-α due to excessive inflammatory responses to LPS is a cause of endotoxin shock or lethality, we also examined the survival of LPS-injected mice. As expected, the serum concentration of TNF-α was increased three- to fourfold in mice lacking Dok-1 or Dok-2 as early as 1 h after injection as compared with the wild-type controls (Fig. 4 A). Consistently, the mutant mice displayed severe responses to LPS injection at a dose sublethal to the wild-type controls (Fig. 4 B). These results demonstrate that Dok-1 and Dok-2 are negative regulators of innate immunity, at least in the early inflammatory responses to LPS in vivo. Because the Dok-1 or Dok-2 deficiency did not influence TNF-α receptor–mediated activation of MAP kinases and NF-κB in peritoneal macrophages (unpublished data), such a mutation causes hypersensitivity to LPS, but not to TNF-α induced by LPS. It is of note that augmented production of NO, another cause of septic shock (23), was seen in macrophages lacking Dok-1 or Dok-2 (Fig. 1 B).

The recognition of microbial pathogens by cognate TLRs triggers the innate immune response. TLR-mediated signaling involves at least four crucial adaptors, MyD88, TRIF, TIRAP/Mal, and TRAM, having a Toll IL-1 receptor domain, which has the capability to bind an appropriate Toll IL-1 receptor domain in the cytoplasmic region of TLR(s) (24). Recent studies demonstrated that TIRAP and TRAM are essential for TLR4 to recruit MyD88 and TRIF, respectively (25–27). TLR2 also requires TIRAP to recruit MyD88. IRAK-M is a negative regulator of the MyD88-dependent pathway forming a complex with IRAK and IRAK4 to prevent phosphorylation of IRAK and its dissociation from the MyD88–TLR complex, thereby inhibiting NF-κB activation (8). MyD88s acts similarly by blocking the access of IRAK-4 to IRAK (28), and ST2 sequestrates MyD88 and TIRAP from TLR signaling (7). Although these negative regulators play important roles in LPS-mediated signaling in macrophages, there is an inevitable lag period for their induction upon LPS treatment of TLR4 as mentioned earlier. Here, we demonstrated that Dok-1 and Dok-2 are expressed at functional levels before LPS treatment and thus on standby to negatively regulate Erk immediately after the onset of TLR4 signaling. Interestingly, these adaptors are irrelevant to TLR2, TLR3, and TLR9, indicating the specificity of Dok-1 and Dok-2 to TLR4 signaling evoked by LPS, the most potent stimulator in innate immunity. Because TLR2 or TLR9 triggers the MyD88-dependent pathway and TLR3 triggers the TRIF-dependent pathway, each pathway does not suffice to induce the negative function of these adaptors. Although studies are underway to clarify the molecular basis for the Dok-1– and Dok-2–medi-

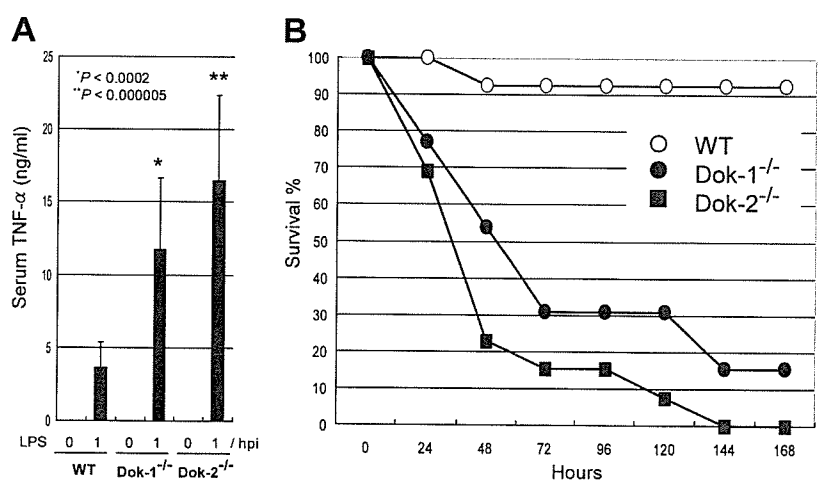

Figure 4. Mice lacking Dok-1 or Dok-2 are hypersensitive to LPS. (A) Serum concentration of TNF-α of 8-wk-old mice at 1 h after injection (1 hpi) with LPS to the peritoneal cavity or before it (0 hpi) was examined with ELISA and shown with SD (n = 7–13). The maximal p-value compared with the wild-type is indicated. (B) Mice at 8 wk of age (n = 13 for each) were injected with LPS as in A and monitored up to 7 d. Data representative of duplicate experiments are shown.